The Dissertation Committee for Colin Averill Certifies that this is the approved version of the following dissertation:

Soil Microbial Community Structure and Allocation Are Critical Drivers of Ecosystem Functioning

Committee:

Christine V. Hawkes, Supervisor

Philip Bennett

Thomas Juenger

Timothy Keitt

Mathew Leibold

Soil Microbial Community Structure and Allocation Are Critical Drivers of Ecosystem Functioning

by

Colin Averill, B.A.

Dissertation

Presented to the Faculty of the Graduate School of

The University of Texas at Austin

in Partial Fulfillment

of the Requirements

for the Degree of

Doctor of Philosophy

The University of Texas at Austin

August 2015

Acknowledgements

My advisor Christine Hawkes has given me tremendous academic freedom to pursue my own independent ideas throughout the course of my Ph.D., and I am truly thankful for her encouragement and feedback over the past five years. I will always be grateful for her willingness to let me pursue the scientific questions that I find most exciting. This work would not have been possible without tremendous support, logistically, financially and academically, from Adrien Finzi. I will always be grateful for his willingness to share his lab space, field sites and unpublished findings as well as personal and professional advice. Marc Andre Giasson was essential in making sure my field and lab campaigns were executed seamlessly, managing countless extractions and chemical assays.

Few complete an advanced degree without an amazing support network, and I need to acknowledge Tiffany Corlin, Sarah Weinstein, Bonnie Waring, Dylan Averill, Trisha Beezup, Eric Benton, Patrick Breen, Jonathan Brennan, Steven Decker, Joshua Gage, Hannah Giauque, Jesse Kees, Stephanie Kivlin, Danielle Mallory, Rory Nolan, Pamela Newman, Kevin Porter, Ian Sutton, Elise Worchel and Aaron Young for being that support. The city of Austin has been an amazing home, and I will never forget its swimming holes, cycling routes and excellent food.

Soil Microbial Community Structure and Allocation Are Critical Drivers of Ecosystem Functioning

Colin Averill, PhD

The University of Texas at Austin, 2015

Supervisor: Christine V. Hawkes

The functioning of terrestrial ecosystems is entirely dependent on the activity of autotrophic primary producers and microbial decomposers, and how they are affected by climate, mineralogy and anthropogenic change. Ecosystem ecology has classically focused on how allocation and community composition of plant primary producers may alter predictions of future ecosystem functioning in the face of environmental change. Little attention has been paid to allocation and community composition of microbial decomposers. The functioning of microbial decomposers has been considered implicitly, in the context of plant traits; primarily plant biomass chemistry. However, soil microbial communities represent a vast diversity of taxa spanning multiple kingdoms of life and an array of functional groups. It is not only likely, but probable that understanding ecological aspects of soil microbial community structure, activity, and allocation will fundamentally change how we understand and predict ecosystem function in the future.

In chapters 1-3 of this dissertation, I explicitly considered how microbial activities varied based on microbial community structure and the resulting impacts for biogeochemical cycling. Specifically, in chapters 1 and 2, I manipulated the relative abundance of symbiotic root fungi to demonstrate that competition between symbionts and free-living decomposers for nitrogen slowed soil carbon cycling. In chapter 3, I

scaled how nitrogen is partitioned between plants, mycorrhizas and free-living decomposer microbes to demonstrate how shifts in microbial community structure could explain how forests productivity is sustained over centuries. In chapter 4, I developed a microbial allocation framework that explicitly considers microbial resource environments. I demonstrated that past microbial allocation frameworks based on plant ecological mechanisms cannot explain allocation patterns of decomposer microbial life.

Throughout this dissertation I attempt to put soil microbial life in an explicit ecological context that challenges current understanding of ecosystem process and will allow for deeper understanding and prediction of ecosystem functioning. Incorporating microbial community structure, allocation, and simple ecological mechanisms into models will improve the predictive power of ecosystem ecology.

Table of Contents

List of Tables

List of Figures

Chapter 1: Ectomycorrhizas slow soil carbon cycling

INTRODUCTION

Carbon (C) storage in terrestrial ecosystems is regulated by C-inputs from net primary production and C-outputs due to decomposition and respiration by microbial decomposers (Schlesinger and Bernhardt 2012). Nitrogen limitation is pervasive in terrestrial ecosystems, and can limit fluxes of carbon (C) through both primary producers and free-living microbial decomposers (Schimel and Weintraub 2003, LeBauer and Treseder 2008). Plants with root-associated ectomycorrhizal (EM) fungal symbionts dominate boreal, temperate, montane and some tropical ecosystems (Read 1991, Torti et al. 2001). These fungi produce enzymes that degrade organic nitrogen (N), which can unlock N trapped in soil organic matter to fuel plant primary production (Rineau et al. 2012). However, by doing so EM fungi may induce or exacerbate N limitation of free-living microbial decomposers. Theoretical models predict that competition between EM fungi and free-living decomposers for N will slow soil C-cycling and increase soil C storage (Orwin et al. 2011), which is supported by a global pattern of increased soil C storage in EM ecosystems (Averill et al. 2014). Yet despite the potential importance for predicting soil and ecosystem C storage, there is still no direct test of the mechanism of action.

Current knowledge is limited by a lack of controlled field experiments that can quantify the degree to which free-living decomposers are N limited, and how much of this limitation may be induced by EM fungi. Isolating mycorrhizal effects under field conditions can be technically challenging. Most field experiments manipulate the

presence and absence of mycorrhizas by coring, trenching, or tree girdling (Högberg and Högberg 2002b, Koide and Wu 2003, Lindahl et al. 2010, Brzostek et al. 2015). However, these experiments cannot control for the disturbance involved in excluding mycorrhizal fungi to measure mycorrhizal effects on soil processes. Because of this, current field experiments cannot separate mycorrhizal effects on free-living microbial activity vs. disturbance effects generating a temporary microbial 'feast' on labile carbon produced from the disruption of fine roots and fungal hyphae. The confounding of disturbance and mycorrhizal effects means there is still no direct test of EM inhibition of saprotrophic activity under field conditions.

We conducted two complementary experiments to test for and quantify EM inhibitory effects on soil C and N cycling. Both explicitly include controls for the disturbance involved in experimentally excluding EM fungi. The 'EM exclusion experiment' tested the effect of EM exclusion on soil C and N cycling over the course of one growing season in an old-growth temperate forest. The 'EM gradient experiment' was conducted over a gradient of EM fungal abundance and over the course of an entire year, allowing us to determine if the effect of EM fungal inhibition scales with the abundance of EM fungi. We measured changes in soil respiration per gram microbial biomass (herein mass-specific respiration) as well as per gram soil. Mass-specific respiration rates have been widely used to better understand soil respiration responses to temperature (Hartley et al. 2008, Bradford et al. 2008, Karhu et al. 2014) and soil moisture (Waring and Hawkes 2014), and allow us to detect shifts in microbial activity due to release from N-limitation. We hypothesized that indicators of both soil C and N

cycling would increase when EM fungi were excluded, compared to disturbance controls, and that this effect would scale with EM abundance.

METHODS

Site description and experimental design: The experiments were conducted at the Harvard Forest in Petersham, MA, USA (42°32' N, 72°11' W). Experimental plots were established within three forest types, which were chosen to represent low, medium, and high EM abundance. Low EM abundance stands were established in girdled, ~130 year old *Tsuga canadensis* stands, originally designed to simulate hemlock wooly adelgid infestation. Since girdling in 2005, the forest has been re-growing as EM black birch. During the current experiment, the girdling treatment had been in effect for 6-7 years. Medium EM abundance stands were established in ~132 year old second growth *Tsuga canadensis* stands used as experimental controls from the girdling treatments. High EM abundance stands were located in 200+ year old, old-growth *Tsuga canadensis* stands. Sites have previously been described in Finzi et al. (Finzi et al. 2014). The old-growth sites were used for the EM exclusion experiment, whereas all sites were used for the EM gradient experiment.

Within each experiment we used a different method to exclude roots and mycorrhizal fungi. The EM exclusion experiment used a fine mesh, while the EM gradient experiment used a trenching technique. In addition to our goal of reducing EM abundance, mycorrhizal exclusion has an obvious disturbance effect. By severing roots and fungal hyphal networks we create a pulse of fresh substrates that may increase microbial activity, which would be confounded with the predicted release from EM

inhibition. We controlled for this disturbance by explicitly incorporating disturbance controls into our design with both methods.

In the EM exclusion experiment we constructed mesh ingrowth bags, filled with sieved organic horizon material from the old-growth, high-EM *Tsuga canadensis* stand. The disturbance control treatment was implemented using in-growth bags constructed of 2-mm fiberglass window screen, which allows entry of fine roots and mycorrhizal hyphae. The mycorrhizal exclusion treatments were made of 1-µm nylon mesh, which excluded both roots and mycorrhizas. In-growth bags (12 x 12 cm) were filled with ~100 g of field moist organic horizon material and sealed at the top. Three replicates of each treatment were installed in each of six plots within the high EM site. Treatments were installed during the first week of June 2013 and harvested the third week of August 2013. Harvested cores were homogenized by hand, roots were removed, and soils were sub-sampled for chemical analyses.

In the EM gradient experiment, four 30 x 30 m plots were established in each of the low, medium and high EM sites as described in Finzi et al. (Finzi et al. 2014). In 2011, trenching was used to experimentally reduce EM abundance using two 60 x 60 cm square trenches per plot. The trenches were dug through the soil organic horizon to 30 cm depth from the top of the mineral soil horizon within each plot. To prevent reentry by roots and fungi, trenches were lined with 2-mm thick plastic and then back filled. In-growth bags of sieved organic horizon material were placed both inside and outside trenches at an equal distance from the trench perimeter. Bags were then incubated for up to 13 months in the field. In-growth bags (12 x 12 cm) were made of ~2 mm nylon

window screen to allow entry by fine roots and mycorrhizal hyphae. Two in-growth bags were placed inside and outside of each trench, resulting in four disturbance control, and four exclusion observations per plot. Bags were harvested from the field in June and August 2012 and transported on ice to Boston University where they were processed within 24 h.

Quantification of ECM abundance using sand-in-growth technique: We used the sand in-growth technique to quantify EM abundance in plots, as described in Wallander et al. (Wallander et al. 2013). Briefly, 50-µm mesh bags (8 x 8 x 1 cm) were filled with ~100 g of acid-washed sand. The 50-µm mesh allows for the in-growth of fungal hyphae, but not roots. Furthermore, because the sand is almost entirely depleted of C, mycorrhizal fungi that receive C from plants dominate. The sand in-growth bags therefore act as a hyphal 'trap', in which EM fungi should survive longer than free-living fungi. Four sand bags were installed in each plot, outside of trenches, in July 2011 and harvested in August 2012. We quantified fungal abundance in sand in-growth bags by extracting and quantifying the fungal biomarker ergosterol.

Ergosterol was extracted and quantified from sand using the methods of Hobbie et al. (Hobbie et al. 2009). In brief, 0.75 g of sand were saponified at 70° C for 90 min in 2 ml methanol and 0.5 ml of 2M NaOH. After saponification, 3 ml of pentane and 1ml of methanol were added. The samples were vortexed, centrifuged briefly, and the upper pentane layer removed by pipette. This step was repeated twice more but with 2 ml of pentane. Pentane collections were dried under either He or N_2 gas, re-dissolved in 1 ml of HPLC grade methanol, and filtered through a 0.45-µm PTFE syringe filter. Samples were

run on a reverse phase column (Allsphere ODS-2 250 mm x 4.6 mm) connected to a Waters 501 HPLC Pump, Waters 717 plus Autosampler and a Waters 486 Tuneable Absorbance Detector (Waters Millipore, Milford, MA, USA). A 20-µl injection was eluted with a mixture of 92% methanol and 8% water at a flow rate of 2 ml min^{-1} and quantified at 282 nm. Ergosterol eluted at ~8.3 min. Two samples returned values an order of magnitude greater than the rest, and were determined to most likely be a result of contamination. These samples were excluded from the final analysis.

Fungal community characterization: Soil subsamples (0.2 g) from each in-growth core were extracted for DNA using a MoBio Power Soil DNA extraction kit (MoBio, Carlsbad, CA) following the manufacturer's instructions. DNA was purified using a MoBio Power Clean Pro DNA cleanup kit (MoBio, Carlsbad, CA) and quantified using a Qubit dsDNA HS Assay Kit (Invitrogen, Eugene, OR). Purified DNA (25ng) extracts were amplified by PCR and sequenced (2 x 250 paired-end) on an Illumina MiSeq V2 at the University of Texas Genome Sequencing and Analysis Facility. The PCR amplifications were performed in triplicate using the ITS1f/ITS2 primer pair (White et al. 1990, Gardes and Bruns 1993). 20 µl PCR reactions contained NEBNext High Fidelity PCR Master Mix at 1x (New England BioLabs, Ipswich, MA, USA), forward and reverse primers at 0.25 µM, and template DNA at 0.5 ng μl^{-1}. Thermocycler settings included an initial denaturation step at 98 °C for 30 s, followed by 12 cycles of denaturation, annealing and extension at 98, 62 and 72°C for 30 s each, and a final extension phase at 72 °C for 5 min. PCR reactions were then purified using Agencourt AMPure Bead XP Purification (Beckman Coulter Inc, Brea, CA, USA). Barcode sequences were attached

using PCR Hyb Barcoded primers synthesized by Integrated DNA Technologies (Coralville, IA, USA) and purified using HPLC.

We used the QIIME pipeline (version 1.7) to assemble paired ends, quality filters sequences, and pick OTUs (Caporaso et al. 2010). OTUs were picked using an open reference strategy using uclust (Edgar 2010). Sequences were first compared to the UNITE reference database of fungal sequences (Kõljalg et al. 2013) and sequences without a match were subsequently clustered *de novo* at a 97% similarity threshold. Chimeric sequences were removed from the data set using Chimera Slayer (Haas et al. 2011). Singletons were removed from the data set. Taxonomy was assigned using the RDP Classifier 2.2 (Wang et al. 2007). We first assigned taxonomy using a curated database provided by Kabir Peay (Talbot et al. 2014), which contained ~122,000 fungal sequences with taxonomy resolved to the genus level. We then assigned taxonomy independently using the UNITE reference database of fungal sequences. If a sequence did not have a taxonomy assignment after searching our database of sequences assigned to genus level, but was assigned taxonomy based on the UNITE sequence database, then we included the UNITE taxonomy assignment in our final taxonomy table. All OTUs that did not match to the kingdom Fungi were removed. After OTU assignment and removal of non-fungal OTUs, samples varied from 33670-252534 read/sample, with a mean of 121164.4 reads/sample. We assigned EM status based on whether an OTU belonged to a known EM or saprotrophic genus following Tedersoo et al. (Tedersoo et al. 2014). EM relative abundance within the fungal community was calculated by dividing the number of EM sequences by the total number of fungal sequences.

Ratio of fungi to bacteria: Quantitative PCR (qPCR) was performed to determine relative abundances of fungi and bacteria using the same DNA extracts described above. We used the 5.8S/ITS1f primer pair for fungi, and the Eub338/Eub518 primer pair for bacteria as described in Fierer et al. (Fierer et al. 2005). qPCR reactions were performed in triplicate with SYBR Green PCR Master Mix (Life Technologies, NY, USA) using a ViiA7 Real-Time PCR system (Life Technologies, NY, USA). Each 25 µl reaction contained SYBR Green PCR Master Mix at 1x, forward and reverse primers at 0.5 µM, and 2.5 ng DNA. Standards were generated by cloning the ITS region of *S. cervisiae* or the 16S region of *E. coli* into puc57 plasmid vectors. Plasmid vectors were constructed by GENEWIZ, Inc. (NJ, USA). Product specificity was verified by melting curve analysis and gel electrophoresis. Fungal to bacterial (F:B) ratios were calculated based on the number of ITS and 16S copies detected in each sample.

Soil and microbial biomass C and N pools: Inorganic N concentrations were determined from 10 g soil extracted with 2 M KCl using the methods of Shepherd et al. (Shepherd et al. 2001). Ammonium and nitrate concentrations were determined colorimetrically in microplates following standard protocols (Sims et al. 1995, Doane and Horwath 2003). Extractable organic N in KCl extracts was measured in microplates using the OPAME method (Jones 2002). To determine total soil C and N, soils were dried at 100°C to constant mass, ground with mortar and pestle, weighed, wrapped in tin capsules and run on an NC2500 Element Analyzer for total C and N (CE Elantec, Lakewood, NJ, USA). Gravimetric soil moisture was measured on 5 g soil subsamples dried for at least 24 h at 100°C.

Microbial biomass was quantified using chloroform fumigation and extraction with 0.5M K_2SO_4 (Vance et al. 1987). Control samples were immediately extracted in 50 ml centrifuge tubes. Fumigation was performed by placing a cotton ball within the centrifuge tube, pipetting 3 ml of chloroform onto the cotton ball, capping the tube, and then incubating the samples in the dark for 7 d (Wallenstein et al. 2006). After incubation samples were vented and then extracted. Organic C and N content of microbial biomass extracts was determined with an Apollo 9000 TOC/TN Analyzer with autosampler (Teledyne Tekmar, Mason, Ohio, USA) using arginine as a standard. We applied correction factors from Vance et al. (Vance et al. 1987) to scale from extractable microbial C and N to total microbial C and N.

Soil microbial C and N fluxes: Soil respiration was measured by placing 20 g of field moist soil into a 488-mL glass mason jar fitted with a septum for headspace sampling. Soils were allowed to equilibrate for 24 h after being weighed into jars. Three gas samples were taken from each jar over a period of 3 h. CO_2 was measured using a bench top infrared gas analyzer (EGM-4, PP Systems, Amesbury, MA).

We measured the gross proteolytic rate using the assay described in Watanabe and Hayano (Watanabe and Hayano 1995) and modified by Lipson et al. (Lipson et al. 1999). Each soil was incubated in 10 ml of 0.5 mmol sodium acetate buffer (pH 5.0) with 400 µl of toluene to inhibit microbial uptake of organic compounds. Soils were incubated for 2 h, and assays were terminated by adding 3 mL of trichloroacetic acid. A separate set of controls were extracted immediately to determine initial dissolved organic N concentrations. By adding toluene, the rate at which dissolved organic N builds up in

solution can be measured in the absence of microbial uptake. Gross proteolytic rate was calculated as the difference in dissolved organic N between incubated and control soils, divided by incubation time.

Soil enzyme activities: We measured the activities of four hydrolytic enzymes involved in the decomposition of C and N: beta-glucosidase, cellobiohydrolase, n-acetyl glucosaminidase, and leucine aminopetidase. These were chosen because they are considered important indicator enzymes for understanding microbial function (Sinsabaugh et al. 2008). Soil enzyme activities were measured fluorometrically (German et al. 2011) on frozen (-80°C) soil subsamples. All assays were performed at substrate saturation in order to measure V_{max} following German et al. (German et al. 2011).

Mass-specific respiration: Because EM fungi can represent one third or more of the total soil microbial biomass (Högberg and Högberg 2002a), exclusion of EM fungi may lead to a net decline in total microbial biomass and associated fluxes, even if free-living decomposer biomass has increased, as well as the turnover of soil C. This is because the source of respiration measured with EM-fungi present is a mixture of recent photosynthate fed to EM fungi, and soil organic C processed by free-living decomposers, while the source of respiration when EM fungi are excluded is solely soil organic matter. For this reason, we report both respiration per gram microbial biomass (herein mass-specific respiration) as well as respiration per gram soil. This allows us to capture changes in the rate of soil C turnover due to a comparatively more active microbial biomass. Mass-specific respiration rates have been widely used to better understand soil

respiration responses to temperature (Hartley et al. 2008, Bradford et al. 2008, Karhu et al. 2014) and soil moisture (Waring and Hawkes 2014).

Statistical analysis: Ergosterol concentrations of sand-ingrowth bags were averaged within plot, and then analyzed using ANOVA to test for a relationship with stand age. We analyzed all other response variables in a mixed effects framework using the lme function in the nlme package for R-statistical software (Pinheiro et al. 2014, R Core Team 2014). Plot was coded as a random effect so that treatments and disturbance controls from within the same plot were paired (Gelman and Hill 2007). We tested for main effects of stand age and mycorrhizal exclusion (trenching), as well as an interaction between the two predictors in the EM gradient experiment. When interactive effects were not significant predictors for a response variable, we only included main effects. If interactive effects were significant we tested for differences between trench and control treatments within each site using the glht function within the multcomp package in R (Hothorn et al. 2008). In the EM exclusion experiment we tested for main effects of mycorrhizal exclusion.Furthermore, the 1-µm mesh used to implement mycorrhizal exclusions significantly increased gravimentric soil moisture by ~5% relative to controls. To account for this we fitted all models with soil moisture as a covariate.

Fungal community composition was analyzed as a function of site, trenching treatment, plot, and their interaction with PERMANOVA using the adonis function in vegan (Oksanen et al. 2015) in R (R Core Team 2014) based on Bray-Curtis dissimilarities calculated from an abundance matrix of fungal OTUs. Results were visualized with non-metric multidimensional scaling (NMS) in PC-Ord (McCune and

Mefford 2011).

RESULTS

In the first experiment, where EM fungi were excluded over the course of the 2013 growing season, we found that the exclusion of EM fungi increased soil C-respiration by 39% (Figure 1.1a) and mass-specific soil respiration by 64% (Figure 1.1b). The exclusion of EM fungi was associated with multiple signals of increased microbial N availability, including a 185% increase in the N-mineralization rate (Figure 1.1c), and a 38% decline in mass-specific proteolysis (Figure 1.1d), an indicator of microbial allocation to N-acquisition. Despite the decline in microbial allocation to N-acquisition, overall microbial allocation to decomposition increased when EM fungi were excluded, resulting in a 87% increase in mass-specific enzyme activity (Figure 1.1e).

In the second experiment, ergosterol concentrations within sand in-growth bags increased significantly across the stand age gradient ($p<0.05$, Figure 1.2a), indicating an increase in EM abundance. EM relative abundance within the fungal community and F:B ratios tended to increase along the stand age gradient (Figure 1.2b). Trenching reduced both the relative abundance of EM sequences and F:B ratios compared to controls ($p<0.05$ in both cases, Figure 1.2c), resulting in conditions similar to the low abundance EM black birch stands (Figure 1.2b).

Fungal community composition shifted across the gradient from low to high EM sites, with EM exclusion communities in each site representing a subset of the total fungal community composition (Figure 1.3). Fungal communities differed across the EM gradient sites (F = 5.27; partial r^2=0.099, P < 0.001) and between the EM exclusion

treatments (F = 4.59; partial r^2=0.043, P < 0.001) based on PERMANOVA. Trenching also had a unique effect in each site (F = 2.05; partial r^2=0.038, P < 0.001), largely resulting in subsets of the local fungal community. The first two axes captured 31% of the variation. Axis 1 was correlated with % soil C (r^2 = 0.41; P < 0.001).

Across the EM gradient, Microbial biomass C:N was highest at the high EM sites (p<0.01, Figure 1.4a). Trenching did not alter biomass C:N. Mass-specific proteolytic rates increased across the gradient and were highest in the high EM sites (p<0.01, Figure 1.4b). Microbial biomass per unit soil C was lowest in high EM sites (p<0.001, Figure 1.4c). There was a significant interaction between site and treatment such that biomass per gram soil C declined in trenches within the low EM sites (p<0.001) but not the medium or high EM sites. There was a significant decline in mass-specific proteolytic rates in trench treatments (p<0.01, Figure 1.4d). Mass-specific C and N degrading activities (BG+CBH and NAG+LAP) followed the same pattern across sites, with old-growth sites having the highest mass-specific activities (p<0.05). Mass-specific C-degrading enzyme acitivity significantly increased in trenches (p<0.05, Figure 1.4e). There was no effect of trenching in mass-specific N-degrading enzyme activity.

Mass-specific respiration was highest in the high EM sites (p<0.05). There was an interaction between site and trenching treatment such that mass-specific respiration increased within the trenches only at the high EM site, but not medium or low EM site (p<0.05, Figure 1.5).

DISCUSSION

Multiple lines of evidence support the emerging idea that EM fungi significantly contribute to the decomposition and selective mining of organic N from soils (Lindahl et al. 2010, Rineau et al. 2012, Bödeker et al. 2014, Lindahl and Tunlid 2015). This leads to the prediction that selective decomposition and uptake of organic N by EM fungi will drive N-limitation of free-living decomposers, slow soil C-respiration and increasing soil and ecosystem C-storage (Orwin et al. 2011). Here we demonstrate that EM-saprotroph competition is occurring under field conditions, slowing both the soil C and N cycles. Exclusion of EM fungi increased soil C-respiration and N-mineralization compared to disturbance controls, shifted microbial allocation to decomposition, and resulted in a more bacteria dominated community. Furthermore, EM inhibition of soil C and N cycling was limited to old-growth temperate forests where EM fungi were greatest in abundance. This field experiment validates a novel mechanism of soil C stabilization, and implies that future changes in EM abundance in response to N-deposition, warming, elevated CO_2 and aggrading forests will alter the strength of the EM competitive interaction, and the magnitude of the C-sink maintained by EM-competitive interactions.

Past experiments to exclude EM fungi have been poorly controlled with respect to disturbance, making it difficult to compare the current study with previous findings. Some past work has also observed increases in microbial activity in response to experimental EM exclusion (Gadgil and Gadgil 1971, 1975, Lindahl et al. 2010), while others find indications of both increased and decreased microbial activity upon exclusion of roots and EM fungi (Brzostek et al. 2015). However, none of these experiments

controlled for disturbance caused by the experimental treatments. Hence, prior results showing increases in microbial activity in response to EM exclusion may be an artifact of experimental treatments.

Despite the increases in soil C and N cycling, we observed an overall decline in microbial biomass when EM fungi were excluded in the first experiment (Figure 1.6a) and either a decline in microbial biomass or no change in microbial biomass at the highest EM sites second experiment (Figure 1.6b). This is unsurprising, however, considering that EM fungi can represent one third or more of the total soil microbial biomass (Högberg and Högberg 2002a). Therefore, exclusion of EM fungi may lead to a net decline in total microbial biomass, even if free-living decomposer biomass has increased, as well as the turnover of soil C. This also supports our use of mass-specific respiration, as it allows us to capture changes in the rate of soil C turnover due to a comparatively more active microbial biomass in the absence of EM fungi.

Fungal communities differed across sites along the gradient, and it is possible that EM fungal community composition, rather than EM abundance, drove the response to EM exclusion. Certain community members may be present at the high EM site, driving the EM inhibition effect, which are absent in the low EM site. We cannot rule this possibility out entirely. However, there is limited mechanistic theory about how fungal community composition may lead to a release from competition when certain members are excluded, while there are established mathematical models regarding how this would be generated as a function of EM abundance (Orwin et al. 2011). Future experiments

could be designed to separate these effects, using communities constructed in the laboratory, while manipulating the abundance of EM fungi in experimental trials.

Our design is not perfectly controlled, as there are C inputs from primary productivity present in the root and EM-ingrowth disturbance controls that are absent in the EM-exclusion treatments. Ideally we would create treatments where roots could grow in without EM fungi, and also add EM fungal necromass equal to any EM fungal turnover in the disturbance controls. Because we cannot include these inputs in the EM exclusion treatments, we have likely under-estimated the EM-inhibitory effect on soil C-cycling, as these organic matter inputs would likely further increase soil microbial activity in the EM-exclusion treatments compared to disturbance controls.

This field experiment validates a novel mechanism of soil C storage predicted from ecological theory (Orwin et al. 2011), with the potential to explain the global pattern of elevated soil C storage observed in EM ecosystems (Averill et al. 2014). Changes in plant allocation to EM fungi due to warming, forest age, elevated CO_2, and other global change factors will likely alter the strength of the competitive interaction between EM fungi and free-living decomposers (Garcia et al. 2008, Clemmensen et al. 2013). Positive or negative feedbacks to climate change are possible, depending on whether global change results in a net decrease or increase in the abundance of EM fungi relative to other microbial functional groups in soil. This highlights the need to begin incorporating basic microbial functional groups into global soil C models, similar to how plant functional types have been incorporated into the Community Land Model (Lawrence et al. 2011). Acknowledging and modeling ecological interactions within soil microbial communities,

and in particular with ectomycorrhizal fungi, has the potential to transform understanding of how C is distributed across the Earth.

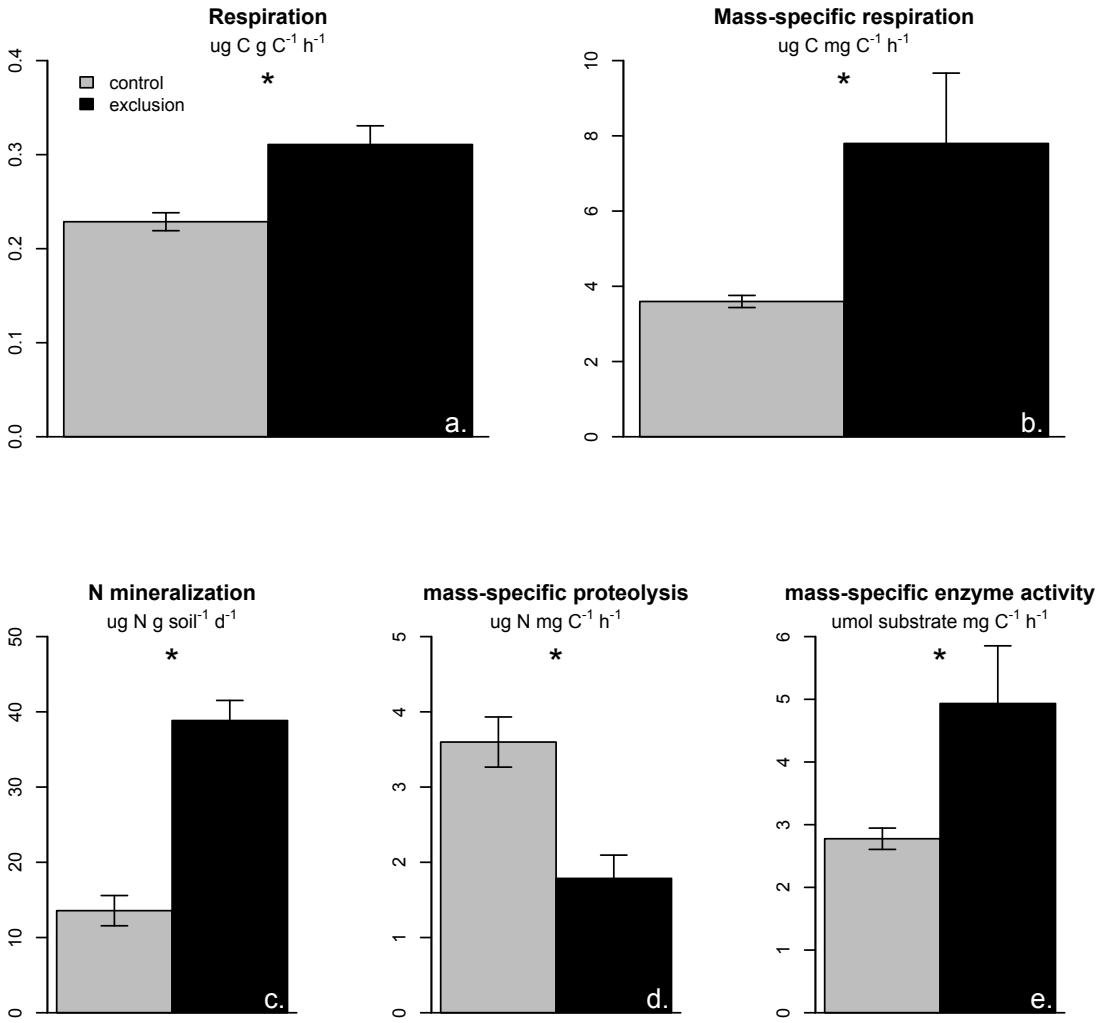

Figure 1.1: Responses in EM exclusion experiment of (a) soil respiration, (b) mass specific soil respiration, (c) net N mineralization, (d) mass-specific proteolytic rate, and (e) mass-specific enzyme activity. All differences significant at $p<0.05$.

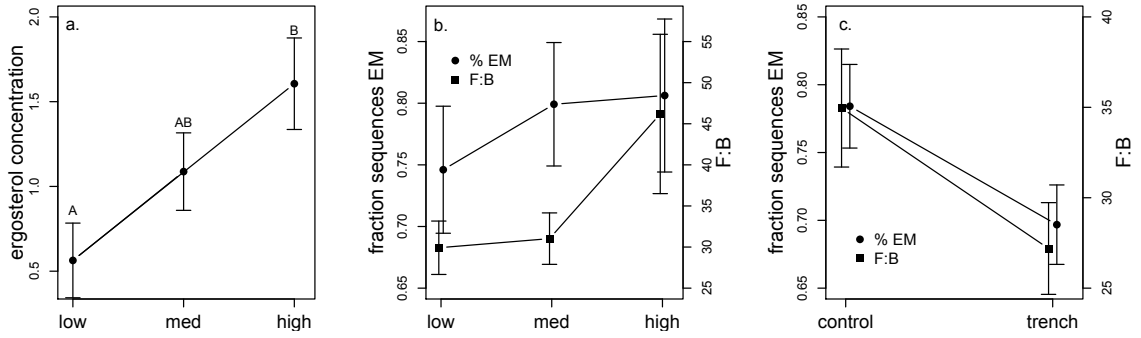

Figure 1.2: Microbial community patterns across sites and trenches in experiment 2. (a) Ergosterol concentrations from sand-ingrowth bags are plotted by site in units of μg ergosterol g^{-1} sand. (b) Relative abundance of EM sequences and F:B by site. Fraction of sequences EM is calculated as the number of fungal sequences designated EM divided by the total number of fungal sequences from each sample. F:B is based on the number of copies of fungi and bacteria from qPCR assessment. (c) Responses of EM sequence relative abundance and F:B to EM exclusion by trenching. Differences are significant at $P < 0.05$.

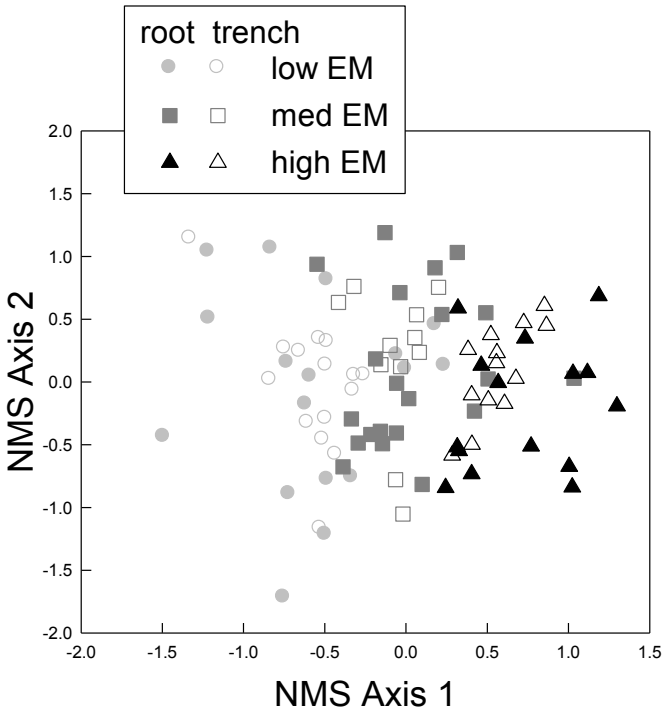

Figure 1.3: Non-metric multidimensional scaling ordination of fungal communities based on ITS sequences from sites across the EM gradient, including both control and trenched samples. Fungal communities were significantly different by site and treatment, with mycorrhizal exclusion treatments representing a subset of the total fungal community at each site ($P < 0.001$).

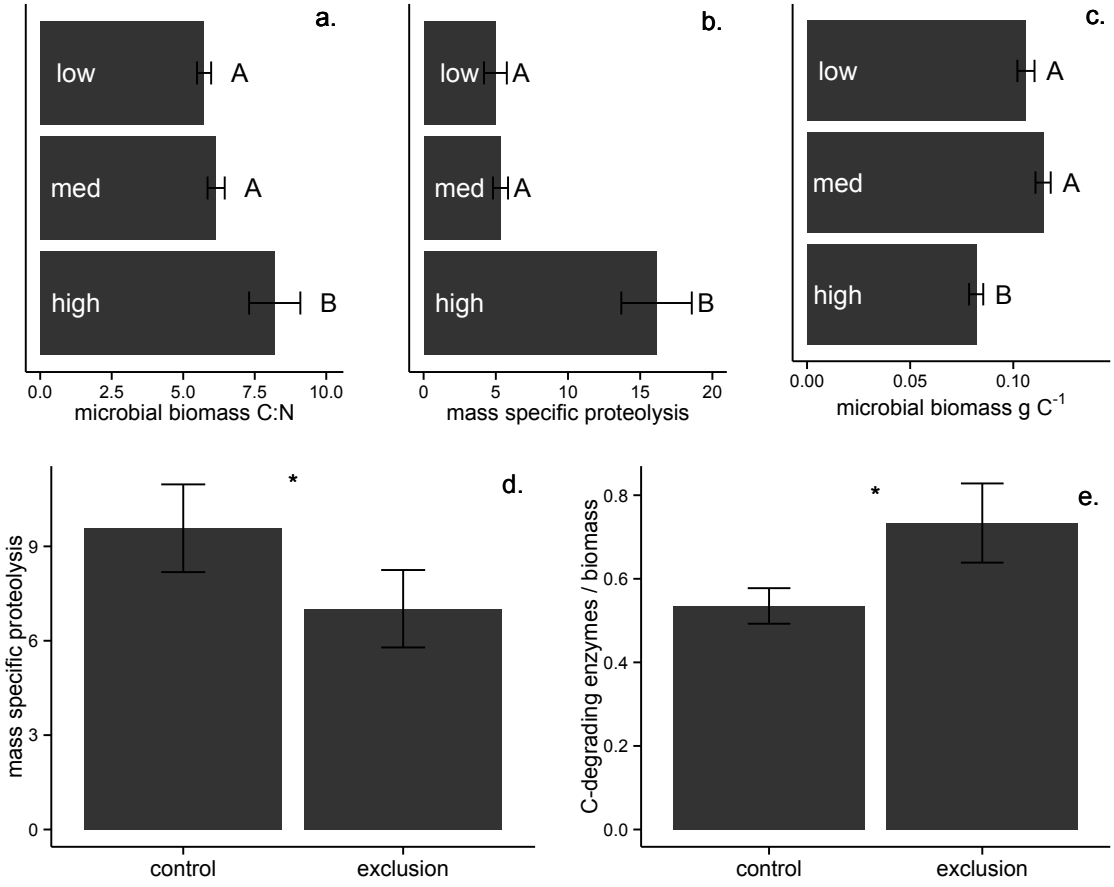

Figure 1.4: Allocation patterns and responses in the EM gradient experiment: Low, medium and high are in reference to the abundance of EM fungi within the soil microbial community in Experiment 2. (a) Microbial biomass C:N across sites (g C g N^{-1}), (b) Mass-specific gross proteolytic rate (ug N mg C-1 h^{-1}), (c) Microbial biomass C per g soil (mg C g C^{-1}), (d) Mass-specific gross proteolytic rates (ug N mg C^{-1} h^{-1}) (e) Mass-specific C-degrading enzyme concentrations (umol mg C^{-1} h^{-1}). Letters and asterisks indicate significant differences ($p<0.05$).

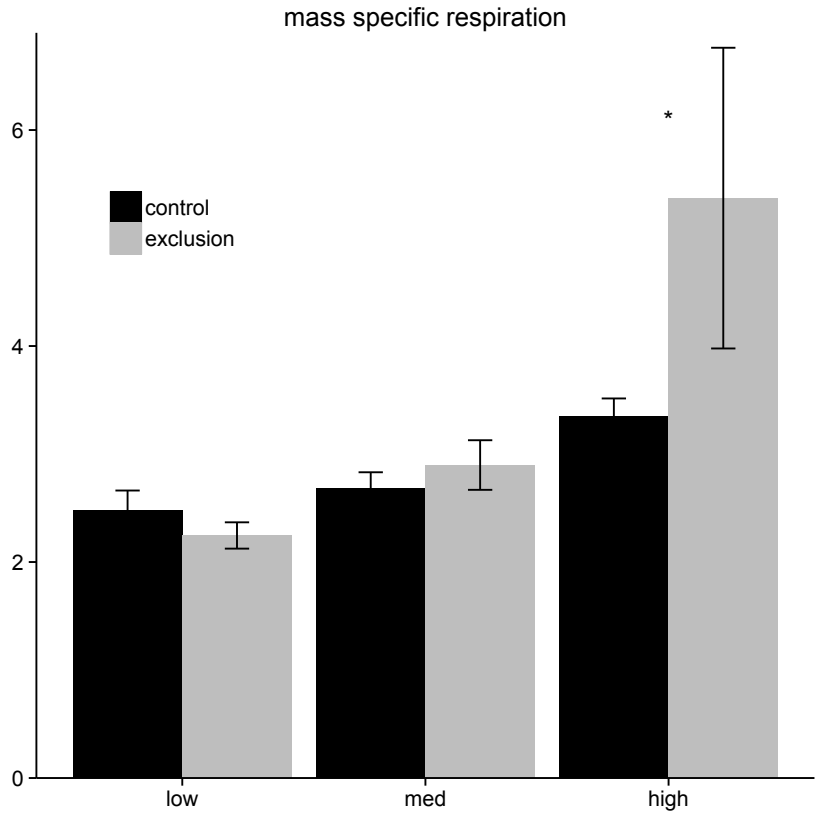

Figure 1.5: There was a significant interaction between mass-specific respiration (ug C mg C^{-1} h^{-1}) and site in the EM gradient experiment, such that increases in mass-specific respiration in response to EM exclusion by trenching were limited to the highest abundance EM site ($p<0.05$).

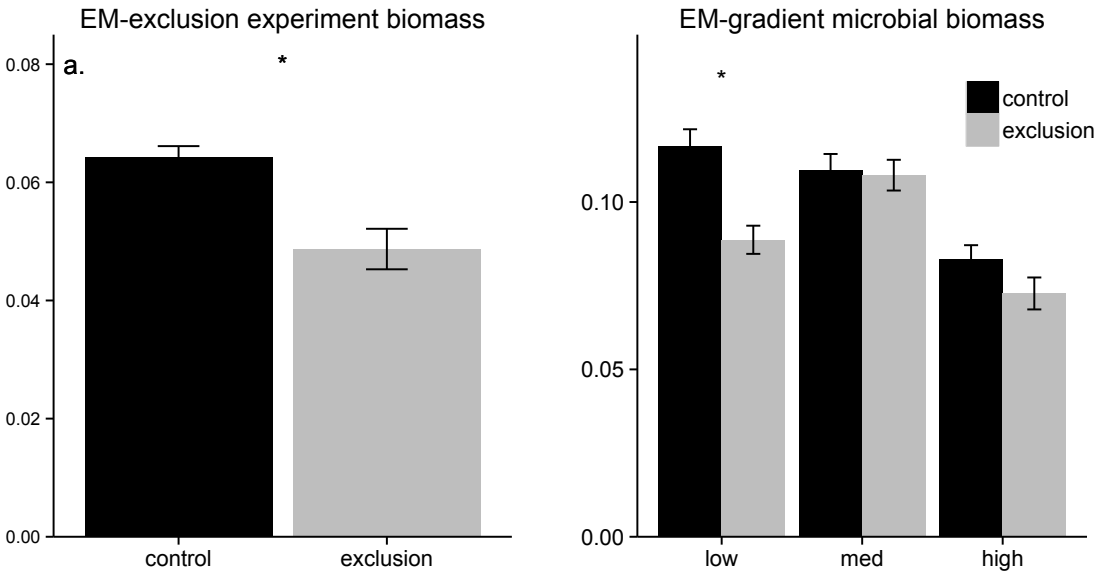

Figure 1.6: Changes in microbial biomass in each experiment (mg C g C^{-1}). Asterisks denote significant differences at $P < 0.05$.

Chapter 2: Separating the effects of mycorrhizal type and organic matter chemistry on mycorrhiza-decomposer competition

INTRODUCTION

Mycorrhizal fungi are critical plant symbionts, and can dominate below ground microbial communities (Högberg and Högberg 2002, Read and Perez-Moreno 2003). While research on mycorrhizas has long been focused on how the symbiosis affects plant nitrogen (N) and phosphorus (P) nutrition, there is still a limited understanding of how mycorrhizal nutrient uptake alters the activity of free-living decomposers within an ecosystem. Recent work has suggested that divergent nutrient acquisition strategies of ecto- and arbuscular mycorrhizal (EM and AM) fungi may be critically important to understanding mycorrhizal controls over soil carbon (C) cycling and storage (Orwin et al. 2011, Phillips et al. 2013, Averill 2014). Ectomycorrhizal fungi degrade organic matter by producing N-degrading enzymes (Read and Perez-Moreno 2003, Rineau et al. 2012). By selectively mining organic N, EM fungi can eventually induce N limitation of free-living decomposers (Orwin et al. 2011, Lindahl and Tunlid 2015), driving slower soil C cycling and increased soil C storage as a result (Gadgil and Gadgil 1971, 1975, Averill et al. 2014). In contrast, AM fungi lack the ability to produce N-degrading enzymes (Read and Perez-Moreno 2003) and have been shown to accelerate soil C turnover by stimulating free-living decomposer communities, likely by means of a priming mechanism (Hodge and Fitter 2010, Cheng et al. 2012). The biogeochemical consequences of different mycorrhizal associations implies that ecosystems dominated by EM vs. AM will have divergent C-cycling responses to global changes such as N-

deposition, elevated CO_2 and warming (Treseder and Allen 2000, Clemmensen et al. 2006).

Despite the growing appreciation of potential mycorrhizal controls over biogeochemical cycles, current knowledge is limited by a lack of controlled field experiments, and confounding between mycorrhizal type and plant input litter chemistry. Isolating mycorrhizal effects under field conditions can be technically challenging. Most field experiments manipulate the presence and absence of mycorrhizas by coring, trenching, or tree girdling (Högberg and Högberg 2002, Koide and Wu 2003, Lindahl et al. 2010, Brzostek et al. 2015). However, these experiments cannot control for the disturbance involved in excluding mycorrhizal fungi to measure mycorrhizal effects on soil processes. Because of this, current field experiments cannot separate mycorrhizal effects on free-living microbial activity vs. disturbance effects generating a temporary microbial 'feast' on labile carbon produced from the disruption of fine roots and fungal hyphae. The confounding of disturbance and mycorrhizal effects means there is still no direct test of EM inhibition of saprotrophic activity under field conditions.

Covariation between plant mycorrhizal type and input litter chemistry has also complicated interpretations of mycorrhizal effects. Ecosystems dominated by AM fungi are typically associated with relatively low C:N, labile plant litter input chemistry, whereas EM-dominated systems are associated with high C:N, recalcitrant litter input chemistry (Read and Perez-Moreno 2003, Phillips et al. 2013). Hence, divergent C and N cycling responses in the presence of AM vs. EM fungi could be argued to be an

interaction with organic matter chemistry, rather than differences in mycorrhizal foraging strategies per se.

To overcome these limitations, we conducted mycorrhizal exclusion experiments in AM and EM forest stands at the Harvard Forest in Petersham, MA. We experimentally controlled for disturbance in our treatments to isolate mycorrhizal effects on soil C and N cycling. The AM and EM sites are also confounded with litter chemistry: AM sites have low C:N, relatively labile plant litter, whereas EM sites have high C:N, relatively recalcitrant litter (Brzostek and Finzi 2011). To account for this confounding, we reciprocally transplanted soils between AM and EM stands to determine if contrasting mycorrhizal in-growth could slow C and N cycling of an AM soil in an EM stand, and vice versa. We had two explicit hypotheses. First, based on previous work (Averill Chapter 1), we predicted that EM removal would result in increased soil saprotrophic microbial activity due to release from competition for N, resulting in greater rates of C and inorganic N cycling in EM exclusions compared to controls. However, we did not expect to see this occur with AM removal in the AM stand. Second, we hypothesized slower cycling of C and N when AM soils were moved to the EM stand compared to home controls, whereas cycling rates of EM soils moved to the AM stand would be accelerated compared to home.

METHODS

Experiment location and site description: The experiment was conducted in an AM-dominated stand of ash (*Fraxinus americana*) and an EM-dominated stand of hemlock (*Tsuga canadensis*) located at the Harvard Forest, Petersham, MA, USA. Soils

are Typic Dystrochrepts (USDA Natural Resources Conservation Service, Web Soil Survey). The two experimental sites within the forest are of similar age and past land-use history; details are provided in Brzostek and Finzi (2011). Experiments were established in six existing replicate, ~200 m^2 circular plots within each forest type (Brzostek and Finzi 2011). Plot selection was based on the following criteria: (1) >80% of the standing basal area was composed of the target tree species, (2) the litter layer was dominated by the target tree species, and (3) the core 80 m^2 circular area of the plot only contained the target tree species.

Experimental design: We used two approaches: (1) mycorrhizal exclusion and disturbance control treatments within each site and horizon to test for a saprotrophic release from competition for N with mycorrhizas, and (2) reciprocal transplants of AM mineral soils into the EM stand, and vice versa, to determine if the presence of AM or EM fungi changed the activity of free-living decomposers, while controlling for soil chemistry. We controlled for disturbance effects by equally disturbing both control and exclusion soils. Exclusion and disturbance control treatments were implemented in mineral soils for the AM-ash and EM-hemlock stands, as well as in the EM-hemlock organic horizon (there was no organic horizon present in the AM stand). The reciprocal transplant treatment was not imposed in the EM organic horizon due to the lack of a corresponding AM organic horizon.

Soils for constructing treatment cores were collected from each plot in May 2013. Mineral soils were sieved to 2 mm, and organic horizons to 4 mm. Soils were homogenized within stand type and horizon, but across plots, and then packed into

experimental treatment cores. The disturbance control and reciprocal transplant treatments were implemented using in-growth cores constructed of 2-mm fiberglass window screen, which allows entry of fine roots and mycorrhizal hyphae. The mycorrhizal exclusion treatments were made of 1-μm nylon mesh, which excluded both roots and mycorrhizas. Mineral soil cores (15-cm length by 6-cm width) for disturbance control and reciprocal transplant were filled with 120 g of field moist soil and sealed at the top. Organic horizon bags (12 x 12 cm) for disturbance control were filled with ~100g of field moist organic horizon material and sealed at the top. Soil cores were installed over two days during the first week of June 2013 and harvested over two days during the third week of August 2013. Harvested cores were homogenized by hand, roots were removed, and soils were sub-sampled for measurement of soil C and N, microbial biomass C and N, respiration, enzyme activities, and net N mineralization.

Soil and microbial biomass C and N pools: Inorganic N concentrations were determined from 10 g soil extracted with 100 ml 2 M KCl. Ammonium and nitrate concentrations were determined colorimetrically in microplates following standard protocols (Sims et al. 1995, Doane and Horwath 2003). Extractable organic N in KCl extracts was measured in microplates using the OPAME method (Jones 2002). To determine total soil C and N, soils were dried at 100°C to constant mass, ground with mortar and pestle, weighed, wrapped in tin capsules and run on an NC2500 Element Analyzer for total C and N (CE Elantec, Lakewood, NJ, USA). Gravimetric soil moisture was measured on 5 g soil subsamples dried for at least 24 h at 100°C.

Microbial biomass was quantified using chloroform fumigation and extraction with 0.5M K_2SO_4 (Vance et al. 1987). Unfumigated control samples were immediately extracted in 50 ml centrifuge tubes. Fumigation was performed by placing a cotton ball within the centrifuge tube, pipetting 3 ml of chloroform onto the cotton ball, capping the tube, and then incubating the samples in the dark for 7 days (Wallenstein et al. 2006). After incubation samples were vented and then extracted. Organic C and N content of microbial biomass extracts was determined using an Apollo 9000 TOC/TN Analyzer with autosampler (Teledyne Tekmar, Mason, Ohio, USA), using arginine as a standard. We applied correction factors from Vance et al. (1987) to scale from extractable microbial C and N to total microbial C and N.

Microbial activities: Soil respiration was measured by placing 20 g of field moist soil into a 488-ml mason jar fitted with a septum for headspace sampling. Soils were allowed to equilibrate for 24 hours after being weighed into jars. Three gas samples were taken from each jar over a period of three hours and CO_2 was measured using a bench top infrared gas analyzer (EGM-4, PP Systems, Amesbury, MA).

We measured the activities of four hydrolytic enzymes involved in the decomposition of C and N: beta-glucosidase (BG), cellobiohydrolase (CBH), n-acetyl glucosaminidase (NAG), and leucine aminopeptidase (LAP). These were chosen because they are considered important indicator enzymes for understanding microbial function (Sinsabaugh et al. 2008). All four soil enzymes were measured using fluorometric techniques (German et al. 2011) on subsamples that were frozen at -20°C until analysis.

All assays were at substrate saturation in order to measure V_{max}, as discussed in (German et al. 2011).

We measured the gross proteolytic rate using the assay described in Watanabe and Hayano (1995) and modified by Lipson et al. (1999). Each soil was incubated in 10 ml of 0.5 mmol sodium acetate buffer (pH 5.0) with 400 ul of toluene to inhibit microbial uptake of organic compounds. Soils were incubated for two hours. Assays were terminated by adding 3 ml of trichloroacetic acid. By adding toluene we can measure the rate at which dissolved organic N builds up in solution in the absence of microbial uptake. Gross proteolytic rate was calculated as the difference in dissolved organic N in incubated vs. un-incubated controls, divided by the number of hours incubated.

We quantified the potential net N mineralization rate by incubating soils for 7 days at lab temperature before extraction with 2M KCl, as described above. Daily net N mineralization was calculated as the difference in inorganic N pool size between incubated and non-incubated soil subsamples divided by the number of days incubated.

Data Analysis: Data were broken into 5 discrete data sets for analysis. First, exclusion treatments were compared to controls, separating data by site and horizon, generating three unique data sets. Analysis was performed using linear mixed effect models, coding plot as a random effect to account for plot-to-plot variation and isolate treatment effects. Mixed effects models were performed using the lme function within the nlme package in R statistical software (Pinheiro et al. 2014, R Core Team 2014).

The reciprocal transplant experiment was analyzed as two separate data sets. The first contained the EM mineral soil disturbance controls (the same controls used in the

previous comparison) and the EM soils that had been moved to the AM stand. The second contained the AM mineral soil controls and the AM soils that had been moved to the EM stand. Data were analyzed using linear regression.

Based on preliminary analysis, differences in soil moisture were confounded with treatments. The 1-μm mesh used to implement mycorrhizal exclusions significantly increased soil moisture in ash mineral soils and hemlock organic horizons by 2-5% compared to controls. Because of this, all models were fit with soil moisture as a covariate.

In all five data sets, we tested for changes in indicators of both soil C and N cycling, as well as differences in the ability of microbes to utilize available soil C resources. Indicators of N cycling were inorganic N pools, N mineralization rates, and gross proteolysis per unit soil N. Indicators of C cycling were mass-specific respiration rates, respiration per unit soil C, mass-specific activities of BG, CBH, NAG and LAP, and microbial biomass pool size per unit soil C. Response variables were log-transformed when necessary to satisfy the assumptions of normality and homoscedasticity. Only significant results are reported at $P < 0.05$.

RESULTS

Mycorrhizal Exclusion: EM organic horizons had strong responses to mycorrhizal exclusion compared to control cores. An increase in inorganic N cycling and simultaneous decrease in organic N cycling was supported by a 192% increase in net N mineralization rate per gram soil N (Figure 2.1A), a 43% decrease in the gross proteolytic rate per gram soil N (Figure 2.1B), and a 24% increase in the log-transformed inorganic

N pool size (Figure 2.1C). Furthermore, an increase in overall microbial activity in the mycorrhizal exclusion was supported by a 47% increase in log transformed mass-specific total hydrolytic enzyme activity (Figure 2.1D), primarily driven by a 250% increase in the log transformed mass-specific activity of BG, a C-degrading enzyme ($P<0.05$, Figure 2.1E). Finally, while we observed a 23% decline in total microbial biomass per gram soil C (Figure 2.1F), there was a 66% increase in mass-specific respiration (Figure 2.1G) and a 37% increase in respiration per gram soil C (Figure 2.1H).

There were no significant effects of mycorrhizal exclusion in the AM or EM mineral soil horizons.

Reciprocal transplants: EM and AM soils showed contrasting N-mineralization responses per unit soil N when reciprocally transplanted. EM mineral soils had 106% higher N-mineralization per gram soil N when moved to the AM stand compared to home, while AM mineral soils moved to the EM stand had 80% lower rates of N mineralization per gram soil N (Figure 2.2).

EM mineral soils moved to the AM stand also had 38% more inorganic N, 45% lower gross rates of proteolysis per gram soil N, and 186% greater mass-specific CBH activity compared to home controls (Figure 2.3A-C). However, there was also a 60% decline in respiration per gram soil C (Figure 2.3D) despite no change in microbial biomass or mass-specific respiration.

AM mineral soil moved to the EM stand also had a increase in CBH activity compared to home controls, but the effect size was over an order of magnitude smaller

than in EM transplanted soils, at 14%. There were no changes in other N cycling metrics, nor were there changes in mass-specific respiration or respiration per gram soil C.

DISCUSSION

Experimental exclusion of EM fungi in the soil organic horizon resulted in substantial increases in C and N cycling by free-living saprotrophic microbial communities. EM fungi in these soils are likely stabilizing a substantial portion of soil C that would otherwise be respired based on observed increases in total and mass-specific C respiration in EM-exclusion treatments. This is consistent with prior work that suggested EM fungi play a critical role in the formation of soil organic horizons (Gadgil and Gadgil 1971, 1975). Moreover, support for EM competition for nutrients inhibiting free-living saprotrophic decomposition is provided by the observed increases in N-mineralization and mass-specific proteolysis when EM fungi are excluded. These results are consistent with theoretical models of EM-saprotroph competition (Orwin et al. 2011), results from Chapter 1, previous exclusion EM exclusion experiments that have resulted in increases in saprotrophic fungal abundance and enzyme production (Lindahl et al. 2010), and reductions in soil organic horizon mass (Gadgil and Gadgil 1971).

As expected, there was no effect of excluding AM fungi in the AM-forest mineral soil horizon. A recent girdling experiment in an AM forest had similar results, with no change in microbial activity in the mineral horizon (Brzostek et al. 2015). However, we also observed no exclusion effect within the EM mineral soil horizon. On the one hand this is surprising as the abundance of EM fungi is generally thought to increase with depth (Lindahl et al. 2007); however C:N ratios of soil also decrease with depth. Thus

competition for N may not be as strong in deeper soils resulting in a less pronounced effect of EM exclusion.

Reciprocal transplant experiments further supported a biotic mechanism underlying the slowing of N cycling in the EM forest, and acceleration of N cycling in the AM forest. Most striking were the dramatic shifts in N-mineralization in transplanted soils. AM soils moved to the EM stand had greatly reduced rates of N-mineralization compared to home, while N-mineralization rates increased when EM soils were moved to the AM stand. This is consistent with the idea that EM fungi slow N cycling in soil, and that this effect can be removed when the soils are moved to an AM system, similar to changes observed when EM fungi were excluded. Furthermore, differences in inorganic N cycling between AM and EM soils cannot be attributed entirely to differences in organic matter chemistry, supporting previous findings with AM fungi (Hodge and Fitter 2010, Cheng et al. 2012).

Despite the compelling changes in N-cycling observed in the reciprocal transplant, the changes in C-respiration were not consistent with EM-induced N-limitation driving changes in soil C-cycling. While no change was observed when AM soils were moved to the EM stand, we found a significant *decline* in C-respiration when the EM soil was moved to the AM stand. This is surprising, and challenging to explain for a number of reasons. We considered the possibility that EM roots and fungi had been subsidizing a large fraction of respiration in mineral soil horizons, however if that was the case then we should have also observed a decline in C-respiration in mycorrhizal exclusion treatments in the EM mineral soil. An increase in N mineralization may have

led to an increase in microbial C use efficiency (*sensu* Cotrufo et al. 2013). However, if such physiological shifts dominated microbial community behavior, then there also should have been an increase in C-respiration when the AM soil was moved to the EM stand and N became more limiting to microbes. Soil microbial communities are more complex than the simple distinctions between saprotrophic vs. mycorrhizal status that we have discussed here, and more complex community shifts may be responsible for the observed changes in soil C respiration (Hawkes et al. 2011).

We note that there was a significant decline in microbial biomass C when EM fungi were excluded in the EM organic horizon soil. We suspect this is driven by the loss of mycorrhizal biomass in exclusion cores coupled without a fully compensatory increase in saprotrophic biomass. Furthermore, the greater activity per unit biomass is consistent with a shift towards a more bacterial dominated community with a faster growth and turnover rate. Previous studies have observed increased bacterial abundance with increasing N availability (Waring et al. 2013), which can lead to a lower steady state biomass pool size due to an increase in the microbial biomass turnover rate. Hence, increased C-respiration is not necessarily in contradiction with a decreased microbial biomass pool size.

Recent theoretical and observational work has suggested that EM-mediated competition between plants and decomposers for soil N can suppress soil respiration and lead to increases in soil C stabilization (Orwin et al. 2011, Averill et al. 2014). Here, we provide experimental evidence under field conditions that this competition does occur in soil organic horizons, and leads to substantial changes in soil C respiration. No inhibitory

effect of AM fungi, or of EM fungi in deeper soil horizons was observed. Reciprocal transplant experiments support the idea that biotic control of soil N cycling is fundamentally different in AM and EM stands, and is independent of soil organic matter chemistry. Taken together, we suggest that this set of experiments provides strong, field-based evidence that EM-induced changes in N cycling mediate an increase in soil C stabilization within ecosystems.

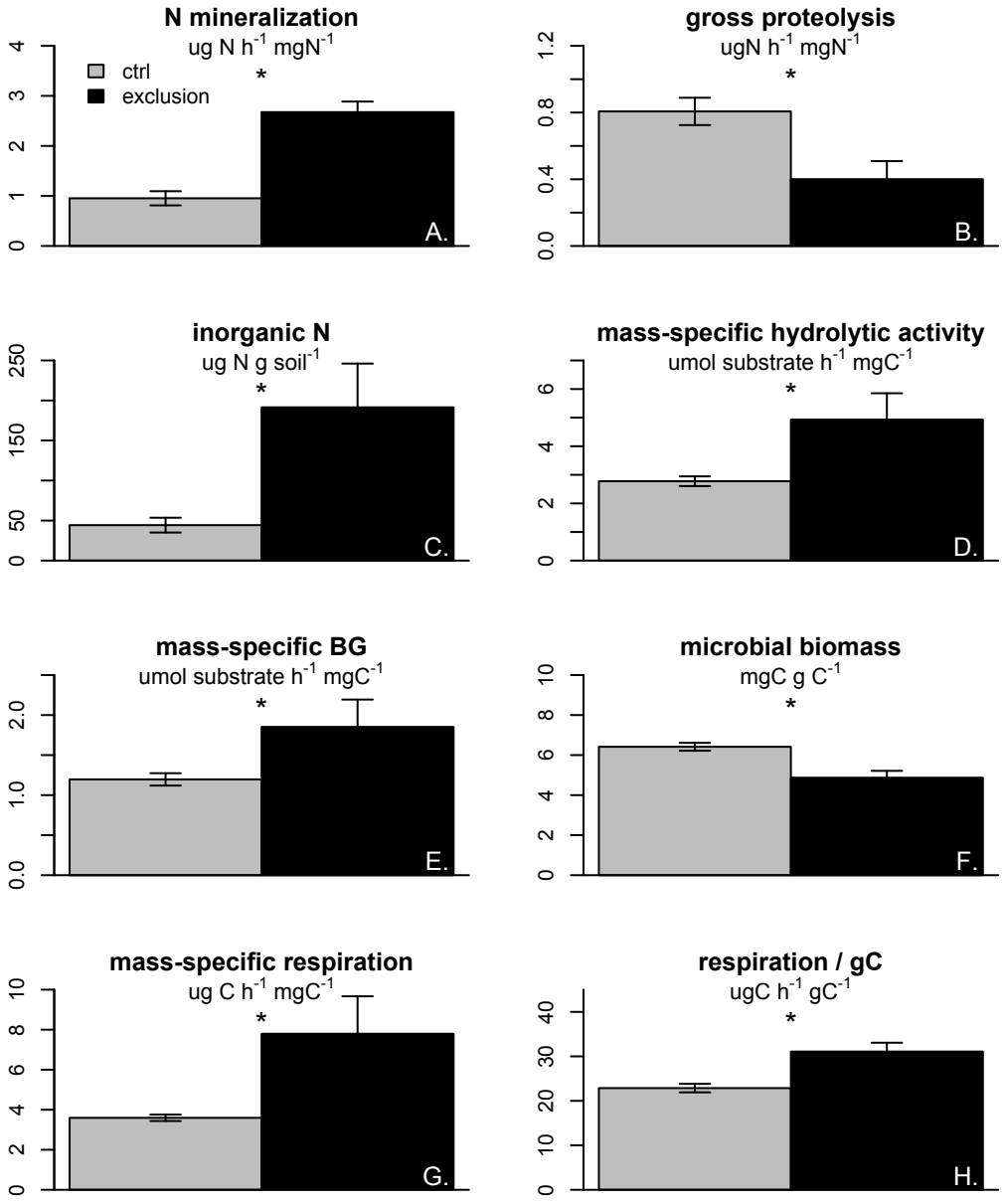

Figure 2.1: Response of ectomycorrhizal soil organic horizons to mycorrhizal exclusion. Disturbance controls are in gray and exclusion treatments are in black. All effects significant at $P < 0.05$.

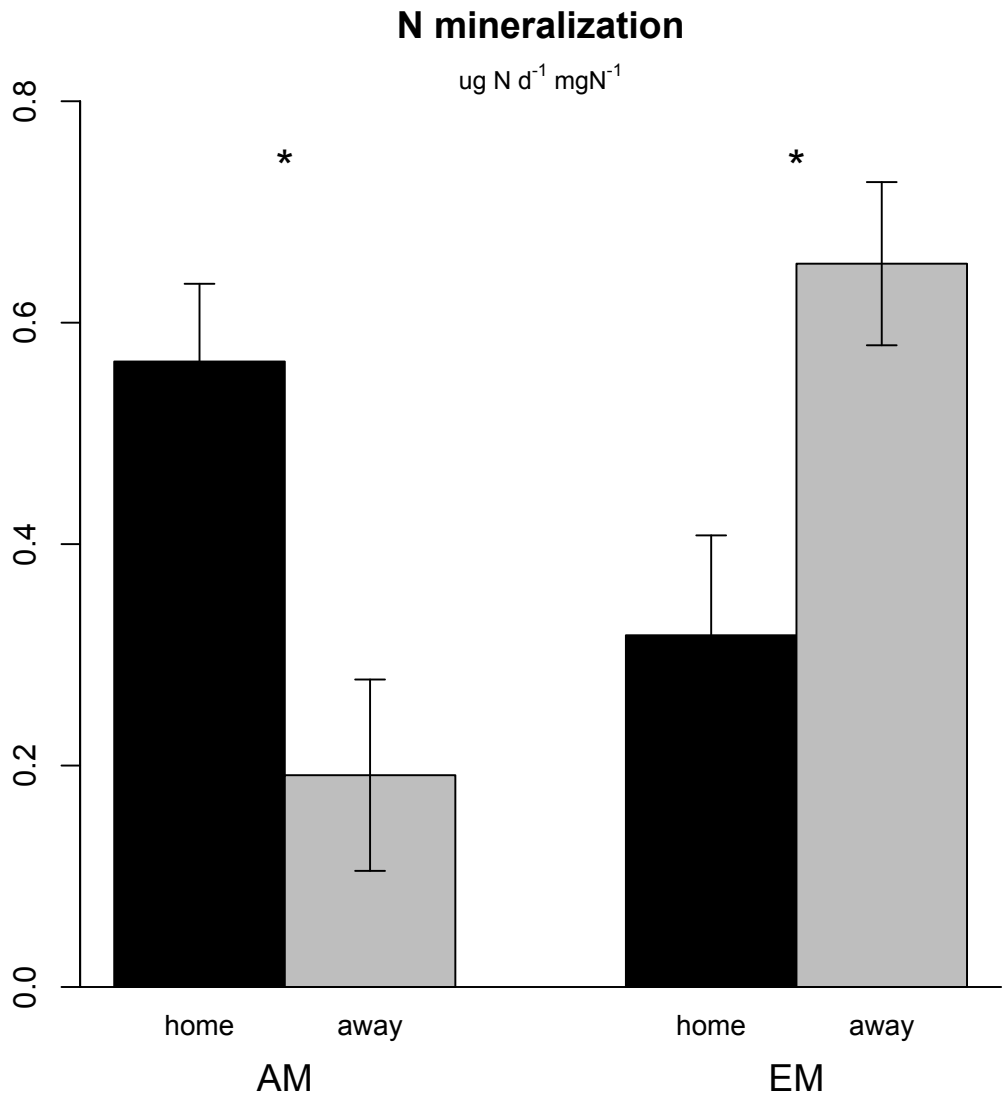

Figure 2.2: Transplant effects on N-mineralization. AM and EM soil responses are separated. 'Home' treatments are AM or EM control cores that have been placed within their stand of origin. 'Away' treatments are AM or EM soils that have been moved to an EM or AM stand, respectively. Asterisks indicate significant differences ($P < 0.05$).

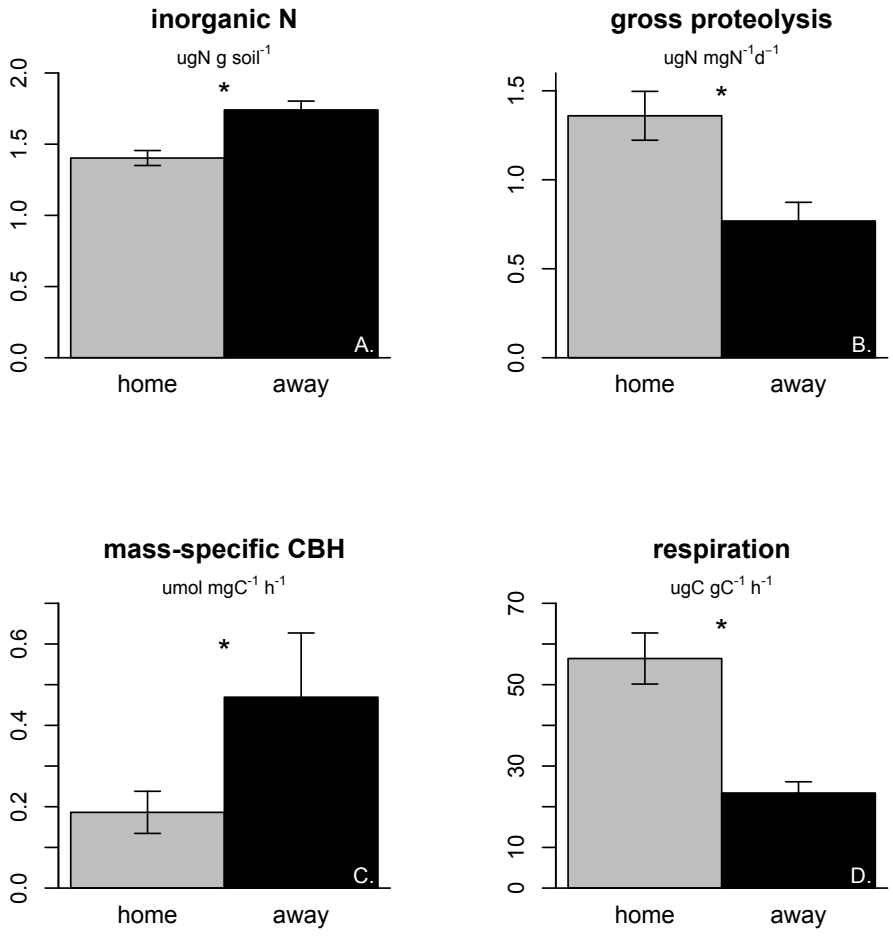

Figure 2.3: Response of EM soil transplants. 'Home' treatments are EM control cores that have been placed within the EM stand. 'Away' treatments are EM soils that have been moved to the AM stand. Asterisks indicate significant differences ($P < 0.05$).

Chapter 3: Microbial nitrogen use efficiency delays progressive nitrogen limitation

INTRODUCTION

Because most terrestrial ecosystems are nitrogen (N) limited (LeBauer & Treseder 2008), N cycling and limitation are critical for a mechanistic understanding of changes in ecosystem carbon (C)-cycling under warming and elevated CO_2 (Melillo *et al.* 2002; Finzi *et al.* 2011), and thus have been implemented in global climate models to constrain future terrestrial C-cycling predictions in response to elevated CO_2 concentrations (Melillo *et al.* 1993; Thornton *et al.* 2009; Wieder *et al.* 2015). The progressive N limitation hypothesis (PNL) has guided the past decade of ecosystem C-N interaction research, and has been used to explain why forest net primary productivity (NPP) declines with age. PNL is also invoked to as a fundamental limit on the response of terrestrial NPP to elevated CO_2 (Luo *et al.* 2004), which currently offsets ~25% of anthropogenic CO_2 emissions (Le Quéré *et al.* 2013). The PNL hypothesis predicts that as plants grow and take up N from soil, N enters plant biomass pools with slow turnover rates, primarily wood, which effectively removes it from the actively cycling pools in the ecosystem. Foliar C:N ratios are also expected to widen, resulting in slower decomposition (assuming C:N is negatively correlated with decomposition). This further slows the ecosystem N cycle, and generates a negative feedback to NPP.

PNL may be delayed if plants respond to elevated CO_2 or decreased N supply by increasing their N use efficiency (NUE), the amount of NPP per unit plant N uptake, or stimulating decomposition of N via allocation to mycorrhizal fungi or rhizosphere

priming of microbial communities (Drake *et al.* 2011; Phillips *et al.* 2011). However, a central assumption underlying putative PNL delay mechanisms is that increases in soil N cycling are required to support increases in plant N uptake. All ecosystem models that represent N-constraints on NPP incorporate this assumption. In the absence of changes in plant NUE or changes in exogenous inputs or outputs of N, NPP can only increase if total rates of N-decomposition increase to support the elevated rate of plant N uptake (Melillo *et al.* 1993; Thornton *et al.* 2009; Wieder *et al.* 2015). This also implicitly assumes that the proportion of microbial N uptake relative to total N decomposition rates within the ecosystem is constant (Figure 1a). However, it is theoretically possible to sustain increased plant N uptake without changes in total soil N cycling, if the increase in plant N uptake comes at the 'cost' of microbial N uptake (Figure 1b).

By producing extracellular enzymes, soil microbes catalyze the conversion of soil organic N into dissolved organic N that can then be used to support both plant and microbial N demand (Schimel & Bennett 2004). If we consider plant N uptake in the context of the microbial N cycle, then we can model plant N uptake as a function of the gross rate at which soil organic N is converted to dissolved organic N and the magnitude of microbial N uptake:

$$Plant\ N\ uptake = Total\ N\ decomposition - Microbial\ N\ uptake$$

This equation makes clear that an increase in plant N uptake could be sustained by an increase in N decomposition *or* a decrease in microbial N uptake, i.e., a change in how N fluxes are partitioned within the ecosystem (Figure 1b).

There are multiple mechanisms that may allow a decline in microbial N uptake while sustaining the same rate of N decomposition. Microbial N uptake m^{-2} yr^{-1} is much larger than plant N uptake when measured at the same scale (Fierer *et al.* 2009; Rousk & Bååth 2011). Hence, a small change in microbial N uptake may sustain a large relative change in the plant N uptake rate. For instance, changes in the fungal to bacterial ratio in the soil microbial biomass can lead to increases in total microbial community C:N and declines in biomass turnover rates, both of which can reduce microbial N uptake (Waring *et al.* 2013). Alternatively, increases in plant allocation to ectomycorrhizal (EM) fungi may also sustain N decomposition rates while reducing total microbial N uptake, as EM fungi are known to produce N-degrading enzymes to catalyze N-turnover (Lindahl *et al.* 2007; Rineau *et al.* 2012) have high C:N ratios (Wallander *et al.* 2003), and may reduce populations of other saprotrophic fungi and bacteria (Gadgil & Gadgil 1971, 1975; Lindahl *et al.* 2007). Hence, multiple aspects of microbial community composition and structure could shift and result in a decline in microbial N uptake for the same rate of N decomposition.

We tested the possibility that changes in the microbial N uptake rate could support increases in plant N uptake without commensurate changes in gross N cycling rates, thus delaying or eliminating PNL. We quantified gross N decomposition, microbial N uptake, and plant N uptake in forests that varied in age from 8 to 200+ years. EM fungal abundance increased along the age gradient (Chapter 1), and we hypothesized that this is the relevant shift in soil microbial community structure that would allow decreases in microbial N uptake to sustain changes in plant N uptake. In order to capture changes in

microbial community structure that may alter N partitioning within the ecosystem, we explicitly measured and modeled bacterial, saprotrophic fungal, and EM fungal growth and N uptake. We had three explicit predictions regarding how N cycling rates would change in relation to each other across the forest age and EM gradient. Specifically:

1. The ratio of plant + mycorrhizal N uptake to total organic N decomposition would increase as plants and associated EM symbionts acquire a greater fraction of the soil gross organic N decomposition flux.
2. The ratio of saprotrophic microbial N uptake to total organic N decomposition would decrease along the gradient as EM fungi become more abundant, increasing microbial C:N ratios and reducing microbial biomass turnover rates, both of which should reduce microbial N demand.
3. The ratio of plant + mycorrhizal N uptake to saprotrophic microbial N uptake should increase as forest age and EM abundance increases.

METHODS

Site Description: The experiment was conducted at the Harvard Forest in Petersham, MA, USA (42°32' N, 72°11' W). Experimental plots were established within three forest types, which were chosen to represent low, medium, and high EM abundance. Low EM abundance stands were established in girdled, ~130 year old *Tsuga canadensis* stands, originally designed to simulate hemlock wooly adelgid infestation. Since girdling in 2005, the forest has been re-growing as EM black birch. During the current experiment, the girdling treatment had been in effect for 6-7 years. Medium EM

abundance stands were established in ~132 year old second growth *Tsuga canadensis* stands used as experimental controls from the girdling treatments. High EM abundance stands were located in 200+ year old, old-growth *Tsuga canadensis* stands. Within each forest stand, four 30 x 30 m plots were established as described in Finzi et al. (2014) and these plots were used here to measure plant and microbial nitrogen uptake, as well as gross rates of N decomposition. All rates were converted to units of g N m^{-2} yr^{-1} to allow comparisons of these fluxes at the same scale.

Plant Nitrogen Uptake: Aboveground plant N uptake values were calculated for each study plot by measuring annual wood and foliage increment for trees, multiplying by tissue %N, and subtracting N recycled via retranslocation (Finzi et al. 2014). Belowground N uptake was calculated by multiplying fine and coarse root biomass N stocks by an annual turnover rate value for each pool. We assumed N retranslocation upon root senescence was trivial (Gordon and Jackson 2000). Fine root turnover rate was based on empirical observations and modeling work done within the Harvard Forest (Gaudinski et al. 2010). The coarse root turnover rate was assumed to be the same as the above ground wood turnover rate. Wood turnover rates were calculated using a steady state assumption by dividing annual wood growth increment by total standing aboveground wood.

Soil Sampling: Within each plot, two samples of the soil organic horizon and mineral soil were taken. Organic horizons were sampled as a 10 x 20 cm monolith. The mineral soil horizon was sampled immediately below the organic horizon using a soil bulk density sampler (5-cm diameter x 15-cm depth). Soils were transported on ice to

Boston University, where they were sieved and processed within 24 h. Mineral and organic horizon soil samples were sieved through 2 mm and 6 mm meshes, respectively. Soils were sampled in June, July, August, and September 2012.

Soil temperature and moisture data were obtained from Finzi et al. (2014). Soil temperature and moisture were measured at 10 cm continuously at all sites from November 2010-November 2011 using thermocouples connected to Campbell 21-X or HK2 data loggers (Campbell Scientific, Inc., Logan, UT). These values were then scaled using an empirical relationship between soil temperature measured at the thermocouple and soil temperature measured at the particular sampling location using a Li-COR 6400 soil temperature probe (LI-COR, Lincoln, NE). Soil moisture was measured hourly at a single plot within each stand type using a 10HS Soil Moisture Smart Sensor (Onset Computer Corporation, Bourne, MA).

Quantifying the gross proteolytic rate: We measured the gross proteolytic rate using the assay described in Watanabe and Hayano (1995) and modified by Lipson et al. (1999). Briefly, each soil was incubated in 10 ml of 0.5 mmol sodium acetate buffer (pH 5.0) with 400 µl of toluene to inhibit microbial uptake of organic compounds. Soils were incubated for 2 h, and assays were terminated by adding 3 ml of trichloroacetic acid. A separate set of controls were extracted immediately to determine initial dissolved organic N concentrations. By adding toluene, the rate at which dissolved organic N builds up in solution can be measured in the absence of microbial uptake. The gross proteolytic rate was calculated as the difference in dissolved organic N between incubated and control soils, divided by incubation time.

Microbial C and N pools: Microbial biomass was quantified using chloroform fumigation and extraction with 0.5M K_2SO_4 (Vance et al. 1987). Unfumigated control samples were immediately extracted in 50 ml centrifuge tubes. Fumigation was performed by placing a cotton ball within the centrifuge tube, pipetting 3 ml of chloroform onto the cotton ball, capping the tube, and then incubating the samples in the dark for 7 days (sensu Wallenstein et al. 2006). After incubation samples were vented and then extracted. Organic C and N content of microbial biomass extracts were determined with an Apollo 9000 TOC/TN Analyzer with autosampler (Teledyne Tekmar, Mason, Ohio, USA) using arginine as a standard. We applied correction factors from Vance et al. (1987) to scale from extractable microbial C and N to total microbial C and N.

Scaling the gross proteolytic rate: The gross proteolytic rate was scaled per gram of soil in the organic horizon and 15 cm of mineral soil based on measured flux rates throughout the growing season, an empirical relationship observed with temperature in these sites (Drake et al. 2013), and a moisture function to allow for diffusion constraints on proteolytic enzyme activity (Davidson et al. 2012). The temperature effect on the potential gross proteolytic rate ($pGPR$), in the absence of diffusion constraints, was modeled based on an empirical relationship:

$$pGPR = e^{a_P * T + b_P}$$

where a_P is a measure of Q_{10}, and b_P is a measure of R_{10}. Previous work has shown that a-values do not vary significantly with season at these sites, while b-values do (Drake et al. 2013). As such, we solved for the b-value within each horizon and time point using

the measured potential gross proteolytic rate, an a_P of 0.684 µg N °T^{-1} $^{-d}$, calculated from Drake et al. 2013. The b-values were then linearly interpolated within plots and horizons across sample dates.

The $pGPR$ was scaled by soil moisture by implementing diffusion constraints on substrate availability from the Dual Arrhenius Michaelis Menten (DAMM) model of Davidson et al. (2012):

$$GPR = pGPR * \frac{S_x}{K_m + S_x}$$

Where S_x is an indicator of the soluble organic N pool, and K_m is the Michaelis-Menten constant for the soluble organic N pool. S_x is modeled as:

$$S_x = S_{x-soluble} * D_{liq} * \theta^3$$

where $S_{x-soluble}$ is the soluble fraction of the total soil organic N pool, D_{liq} is a dimensionless diffusion coefficient of the substrate in liquid phase, and θ^3 is the volumetric water content of the soil, which is driven by empirical data. Finally, $S_{x-soluble}$ was a modeled as:

$$S_{x-soluble} = p * S_{x-total}$$

where $S_{x-total}$ is the concentration of soil N per gram soil, which we measured empirically, and p is the fraction of that N that is made soluble on a daily basis. D_{liq} and K_m parameter values were taken from Davidson et al. (2012). The p parameter, the fraction of total soil N that is potentially soluble, was increased by a factor of four compared to Davidson et al. (2012) as this is the mass weighted C:N ratio of amino acids in soil solution (Friedel & Scheller 2002). We note that changing the value of p by up to

two orders of magnitude altered relative differences in gross proteolytic rate among sites by at most 2%, and did not change significance or qualitative interpretation of results.

Gross proteolytic fluxes were scaled to g N m^{-2} $season^{-1}$ by summing the N flux g $soil^{-1}$ d^{-1} across the growing season and then multiplying fluxes per g soil by the bulk density of a particular soil horizon (g cm^{-3}), the horizons depth (cm), and the unit conversion for area of a meter (10,000 cm^2 m^{-2}, data from Finzi et al. 2014). Values were integrated across the organic and mineral soil horizon to 15-cm depth in the mineral soil.

Scaling microbial biomass N uptake: Microbial biomass N uptake was scaled in the organic horizon and to 15 cm depth in the mineral soil using empirical observations of microbial biomass C and N throughout the growing season, empirical relationships of fungal and bacterial growth with temperature and moisture, and estimates of soil fungal to bacterial ratios (F:B) based on soil C:N ratio and published literature. We first linearly interpolated microbial biomass C and C:N ratios across sampling dates within plots and soil horizons to estimate daily pool sizes of microbial biomass C and N. Microbial biomass N uptake per day is modeled as a mass specific growth function multiplied by the microbial biomass N pool:

$$Microbial\ N_{uptake} = Mass\ specific\ growth * \frac{MB_C}{MB_{C:N}}$$

This calculation assumes steady state, therefore microbial growth equals microbial uptake, and is balanced by losses. Changes in total biomass are driven by the interpolation of empirical microbial biomass C and N values. Mass specific growth is total microbial biomass growth per unit microbial biomass C, MB_C is microbial biomass

C, and $MB_{C:N}$ is microbial biomass C:N. Mass specific growth is then modeled as:

$$Mass\ specific\ growth$$

$$= \left\{ \frac{f(T)_{fungi}}{MB_{C-fungi}} * \frac{F:B}{F:B+1} + \frac{f(T)_{bac}}{MB_{C-bac}} * \left[1 - \left(\frac{F:B}{F:B+1} \right) \right] \right\} * f(M)$$

Where $f(T)_{fungi}$ and $f(T)_{bac}$ are empirical temperature dependent microbial growth C functions for fungi and bacteria, respectively, $MB_{C-fungi}$ and MB_{C-bac} are biomass C observations at a reference temperature from the same temperature study used to parameterize the $f(T)$ relationship, and $f(M)$ is a moisture scalar. These values allow us to convert total growth to mass-specific growth. F:B (g C g C^{-1}) was inferred from soil C:N ratios for each plot and horizon using the empirical relationship described in Waring et al. (2013). Microbial growth of fungi or bacteria was modeled as a function of temperature, $f(T)$:

$$f(T) = (a_T * T + b_T)^2 * bcf$$

Where a_T and b_T are the slope and intercept of the square root transformed relationship between bacterial and fungal growth and temperature for a given soil horizon (Rousk *et al.* 2012, Rousk unpublished data), and bcf is a biomass conversion factor to scale leucine or acetate incorporation rates to bacterial or fungal growth in mg C (Rousk and Baath 2007, Rousk and Baath 2011). The moisture limitation function, $f(M)$, is a logistic function that scales total mass specific growth where:

$$f(M) = 1 + e^{a_M(M-b_M)}$$

Where M is % soil moisture, and a_M and b_M are empirically determined (Iovieno & Baath 2008).

Microbial N uptake fluxes are calculated in mg N g $soil^{-1}$ d^{-1}. To scale fluxes to the stand level, fluxes within a plot were summed across growing season days, multiplied by bulk density (g cm^{-3}) and depth (cm) of the respective horizon (data from Finzi et al. 2014), scaled from cm^2 to m^2 by multiplying by 10,000 (cm^2 m^{-2}), and summed across organic and mineral soil horizon fluxes within plot. Final units are reported as g N m^{-2} yr^{-1}.

Calculating ectomycorrhizal N uptake: EM N uptake was calculated as a fraction of total fungal N uptake on a daily time step where

$$Ectomycorrhizal\ N_{uptake} = Fungal\ N_{uptake} * \%\ Ectomycorrhizal$$

The fraction of soil fungi was determined based on Illumina sequencing of the ITS1 region, then assigning fungi EM or non-EM status at the genus level using the identities presented in (Tedersoo *et al.* 2010). Details of this approach are reported in Chapter 1. EM relative abundance was assumed to be the same in both the organic and mineral soil horizons.

Analysis and Statistics: Changes is N cycling rates were analyzed using ANOVA with site as the main predictor in R (R Core Team 2014). There were four observations per site, for a total of twelve observations. Differences were considered significant at $p<0.05$. Post-hoc comparisons were made using Tukey Honest Significant Differences. We analyzed relative changes in N cycling either explicitly including EM fungal N uptake into the plant N uptake term and modeling saprotrophic N uptake separately, or ignoring EM fungi and comparing relative differences between plant and total microbial N uptake.

RESULTS

There were similar trends across sites in daily gross proteolysis and microbial biomass N uptake throughout the growing season regardless of EM abundance (Figure 3.2-3.3). Behavior was predominantly driven by variations in soil temperature and moisture, which were correlated across sites.

Plant N uptake increased nearly linearly across the gradient, with 85% more N uptake in the high compared to the low EM abundance sites (Figure 3.4a). Plants at both the medium and high EM sites took up more N than the low EM site ($p<0.05$), and plants at the high EM site tended to take up more N than the medium EM site ($p=0.05$). There was no significant change in total microbial N uptake across the gradient (Figure 3.4b). Gross proteolysis over the measurement period declined 31% between low and medium EM sites, and then increased 22% from medium to high EM sites (Figure 3.4c).

When relative fluxes were considered, plant N uptake increased 81% as a proportion of total N cycling (as indicated by the integrated gross proteolytic rate) between low EM abundance and med to high EM abundance sites (Figure 3.5a). Microbial N uptake per unit total N cycling increased 68% from low to medium EM sites, and then declined by 14% in the highest EM sites (Figure 3.5b). There was also a non-significant ($P = 0.132$) trend of increasing plant N uptake relative to microbial N uptake (Figure 3.5c).

We then re-analyzed the data set by separating microbial N uptake into EM fungal and saprotrophic microbial N uptake, and combining plant N uptake with the EM fungal N uptake term. We found plant + EM fungal N uptake increased 88% across the gradient

as a proportion of total N cycling (Figure 3.6a). Saprotrophic uptake of N relative to total N cycling increased 69% from low to medium EM abundance sites and then declined 29% from medium to high EM sites (Figure 3.6b). Plant + EM fungal N uptake increased relative to saprotrophic N uptake across the gradient, with high EM abundance sites having 58% more plant + EM fungal N uptake relative to saprotrophic N uptake compared to medium and low EM abundance sites (Figure 3.6c).

DISCUSSION

Progressive N limitation (PNL) of plant NPP can be delayed during ecosystem succession by either changes in soil N cycling rates or changes in microbial N uptake relative to total N cycling. A change in microbial N uptake relative to total N cycling could be driven by a change in microbial community structure that causes an increase in microbial NUE, and partitioning of N fluxes within the ecosystem. Increases in fungal to bacterial ratios or the abundance of EM fungi could drive this shift (Waring *et al.* 2013). Based on the results of this study, the evidence that EM fungi may play a role in delaying PNL is mixed. Two of our three key predictions are supported. Plant-mycorrhizal N uptake relative to total N cycling increased along the gradient, as did the ratio of plant-mycorrhizal N uptake to saprotrophic N uptake, consistent with the idea that plants and their associated fungal symbionts are acquiring an increasing fraction of the total N decomposition flux, at the 'expense' of saprotrophic microbial decomposers. Indeed, plant N uptake increased linearly with age at our sites (Figure 1a). However, the response of saprotrophic N uptake to the age gradient was not monotonic. Saprotrophic microbes also received a greater fraction of total N cycling when moving from young to medium

aged stands, but this term declined from medium to old stands with high levels of EM fungi. This may be driven by changes in N inputs or outputs to the ecosystems across the gradient, or changes in the relative importance of N mineralization.

Our analysis assumes that external inputs and outputs of N to the ecosystem are trivial compared to internal cycling and uptake fluxes. However, if external inputs are large, then plant and microbial N uptake could *both* increase relative to total N decomposition, as more N is available in the ecosystem than the total N decomposition flux. Similarly, if losses of N from the ecosystem due to leaching or denitrification were large, then *both* plant and microbial N uptake fluxes could decline relative to total N decomposition rates, as a smaller fraction of total N decomposition is retained in the system. We have reason to believe the N losses and inputs from these ecosystems are very small, and cannot explain the patterns observed in the present study. For example, in the low and medium EM forests, N losses due to leaching are on the order of 0.3 g N m^{-2} yr^{-1} (Templer & McCann 2010). Even the smallest observed plant N uptake fluxes in this study are ~10 times greater in magnitude than leaching losses, and both microbial and total N decomposition N fluxes are over 100 times greater. Hence, leaching losses are unlikely to drive the patterns observed in this study. Furthermore, N isotope profiles of NO_3^- leachate at these sites do not indicate that denitrification is a quantitatively important N cycling process within the context of the total N budget of these forests (Templer & McCann 2010). Similarly, N inputs from atmospheric N deposition are low at this site, and comparable in magnitude to the N leaching losses, suggesting that variation in N inputs at these sites are also unlikely to explain the observed patterns

(Templer & McCann 2010).

It is also possible that microbial N limitation is relatively unimportant early in forest succession, so microbes decompose and mineralize a significant amount of DON, and less is retained within the biomass, explaining low ratios of saprotrophic N uptake to total proteolysis at young forest sites. In general ammonium and nitrate concentrations are greatest in the young forest sites, and lower at the older sites, as are ratios of inorganic to organic N detected in soil extractions. This is consistent with past observation of declines in inorganic N cycling rates during secondary succession (Vitousek & Matson 1981). As succession continues, microbial N-limitation begins to set in, explaining the increase in microbial N uptake per unit gross proteolysis between young and medium aged forests. Over the course of another hundred years of ecosystem development there may be ecological pressure for a more N use efficient microbial community as soil N limitation becomes stronger, explaining the decrease in microbial N uptake per unit gross proteolysis between medium and old aged forests. This is supported by the fact that the oldest sites generally have more ectomycorrhizal fungi, higher F:B ratios, and higher microbial biomass C:N (Averill and Hawkes in review). Because we cannot scale soil N mineralization rates through the growing season, we cannot definitively confirm or deny this hypothesis.

Despite the limitation of not having sufficient data on N mineralization, this study demonstrates that increases in plant N uptake do not require increases in soil N cycling rates. Plant N uptake increases across the gradient, while total N cycling *declines*. In the absence of significant inputs/outputs of N to the system, this is not possible unless plants

are getting an increasing fraction of the total N decomposition within the ecosystem. Changes in N partitioning within the ecosystem are therefore a plausible mechanism to delay PNL as forests age, or under elevated CO_2. Support for this is further provided by the Duke Free Air CO_2 Enrichment (FACE) experiment, where sustained increases in NPP occurred for twenty years. This increase was associated with an increase in plant N uptake rates, despite no detectable change in soil N cycling rates at the Duke FACE site (Finzi *et al.* 2007). The increased N uptake of plants under elevated CO_2 may be driven by changes in microbial community structure that lead to a greater N use efficiency of saprotrophic microbes at these sites. Increases in EM fungal abundance have been reported at the Duke experiment (Garcia *et al.* 2008), which would provide a mechanism for a shift in N partitioning at this site. This mechanism has the potential to substantially alter predictions of the future terrestrial C sink stimulated by elevated CO_2, which currently offsets ~25% of anthropogenic CO_2 emissions (Le Quéré *et al.* 2013), and is expected to diminish in the future as ecosystems encounter PNL (Luo *et al.* 2004). Incorporating the N-partitioning mechanism into these models may further delay PNL, and increase the amount of anthropogenic CO_2 emissions that will continue to be sequestered by elevated CO_2 stimulation of terrestrial NPP.

This scaling exercise is not without caveats, and there is uncertainty in the scaling factors used for fungal and bacterial growth in this study. Mass-specific biomass growth rates may change seasonally in this forest, and this will not be captured in our approach. Furthermore, variation in the abundance of EM fungi throughout the growing season cannot be captured, and may alter predictions. Despite these limitations, scaling any

aspect of C or N cycling to ecosystem scale requires assumptions when extending observations at the micro scale to the entire forest. We hope to improve these estimates as more data on microbial growth at multiple scales becomes available.

Future climate projections rely heavily on predictions of terrestrial NPP, which is strongly N limited (LeBauer & Treseder 2008) both as forests age and in how they respond to elevated CO_2 (Finzi *et al.* 2007). The PNL hypothesis provides a conceptual mechanism for the constrained response of NPP under these circumstances. Although the relative importance of different mechanisms that may delay PNL remains debated (Feng *et al.* 2015), we provide evidence that changes in N partitioning among plants, mycorrhizas, and free-living decomposers within the ecosystem contributes to delaying PNL along a 200 year gradient of forest age. Incorporating the N-partitioning mechanism into terrestrial NPP simulations is likely to extend the duration of the terrestrial CO_2 sink stimulated by anthropogenic increases in atmospheric CO_2, and reduce the pool of future CO_2 in the atmosphere.

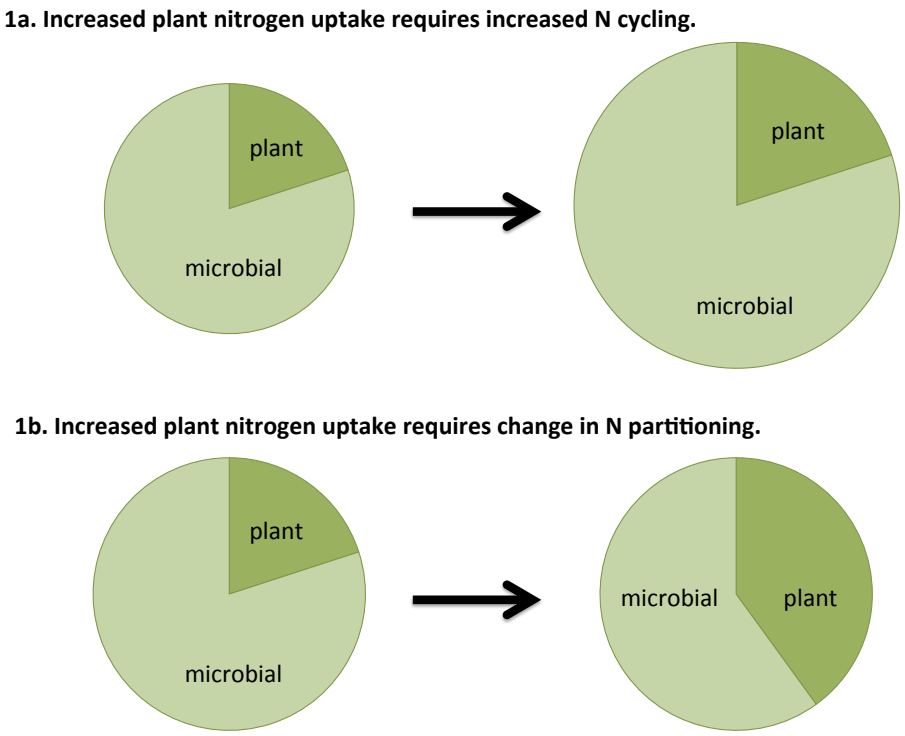

Figure 3.1: Conceptual diagram of N uptake of plants and microbes within an ecosystem. Size of each circle reflects the total amount of soil organic nitrogen turnover within an ecosystem for a given amount of time. 1a) Microbial N uptake is assumed to be a constant fraction of total N decomposition. Increases in plant N uptake require increases in the rate of total N decomposition. 1b) Increases in plant N uptake are possible without changes in total N decomposition. Instead, increased plant N uptake comes at the 'cost' of microbial N uptake.

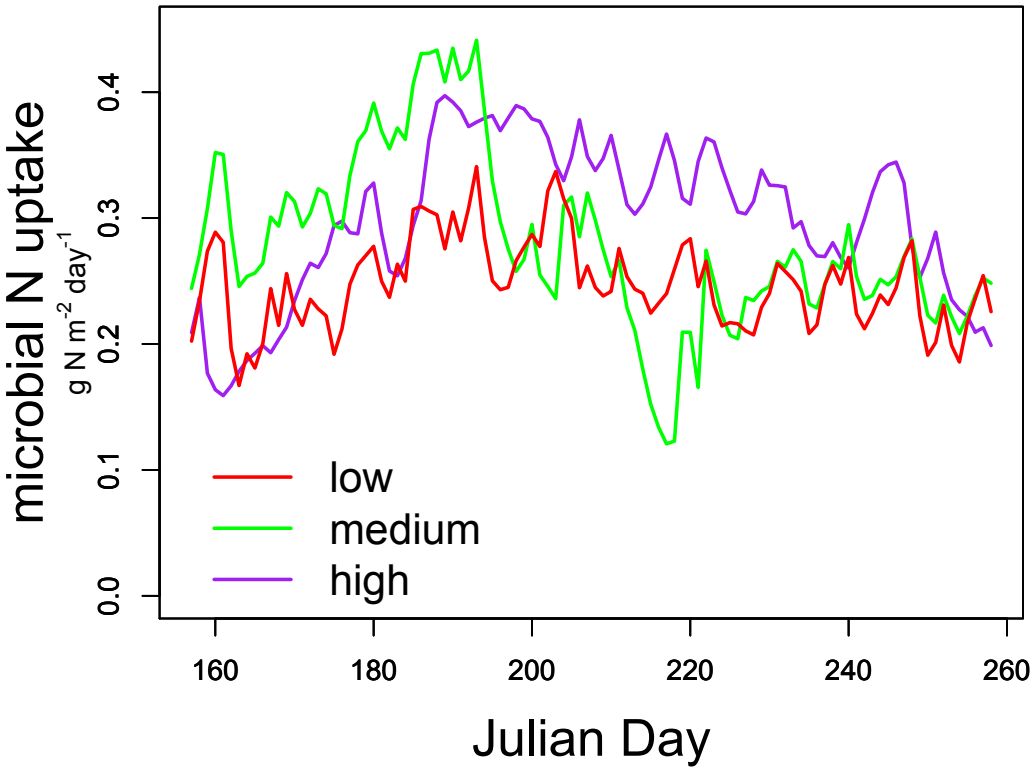

Figure 3.2: Daily gross turnover rate of soil organic N to dissolved organic N over the course of the measurement period. Low, medium, and high indicate levels of EM abundance, corresponding to forest stands that were young (6 years), intermediate (132 years), and old (200+ years), respectively.

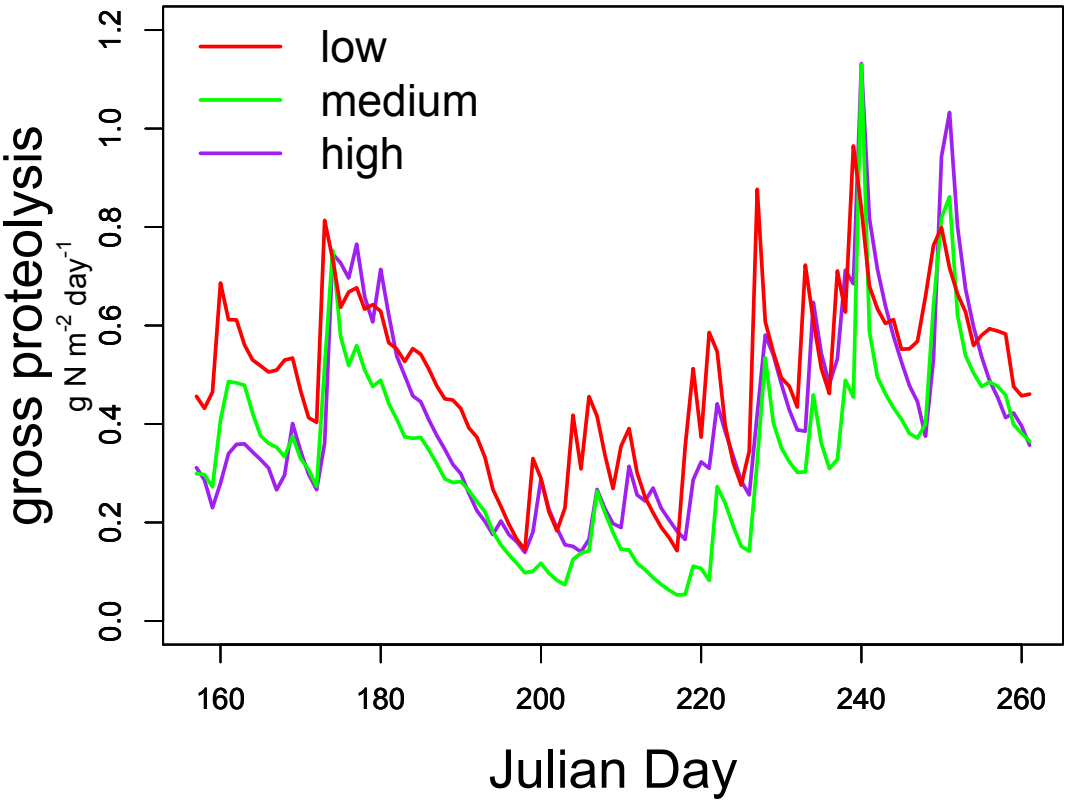

Figure 3.3: Response of EM soil transplants. 'Home' treatments are EM control cores that have been placed within the EM stand. 'Away' treatments are EM soils that have been moved to the AM stand. Asterisks indicate significant differences ($P < 0.05$).

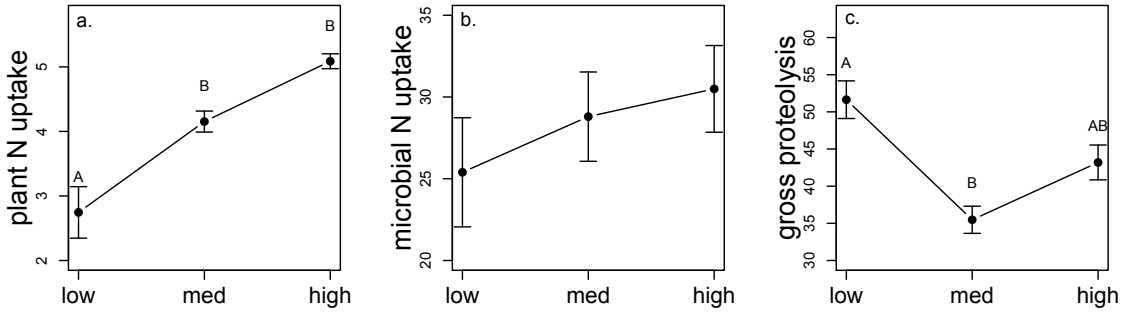

Figure 3.4: Integrated a) plant N uptake b) microbial N uptake and c) total N decomposition over the measurement period. All units are g N m^{-2} yr^{-1}. Low, medium, and high indicate levels of EM abundance corresponding to forest stands that were young (6 years), intermediate (132 years), and old (200+ years), respectively.

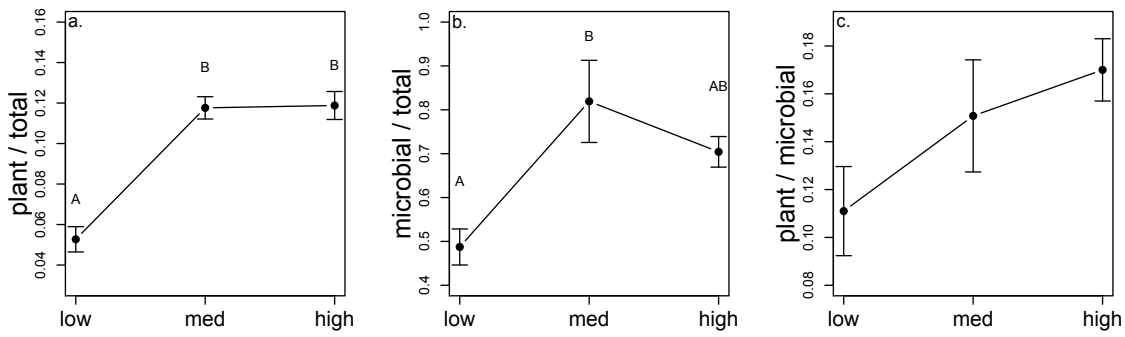

Figure 3.5: Relative fluxes of a) plant N uptake to total N decomposition b) microbial N uptake to total N decomposition and c) plant N uptake to microbial N uptake. All values are unitless, representing ratios of fluxes in units g N m^{-2} yr^{-1}. Low, medium, and high indicate levels of EM abundance corresponding to young (6 years), intermediate (132 years), and old (200+ years) aged stands. Microbial N uptake includes N uptake by free living bacteria and fungi as well as mycorrhizal fungi.

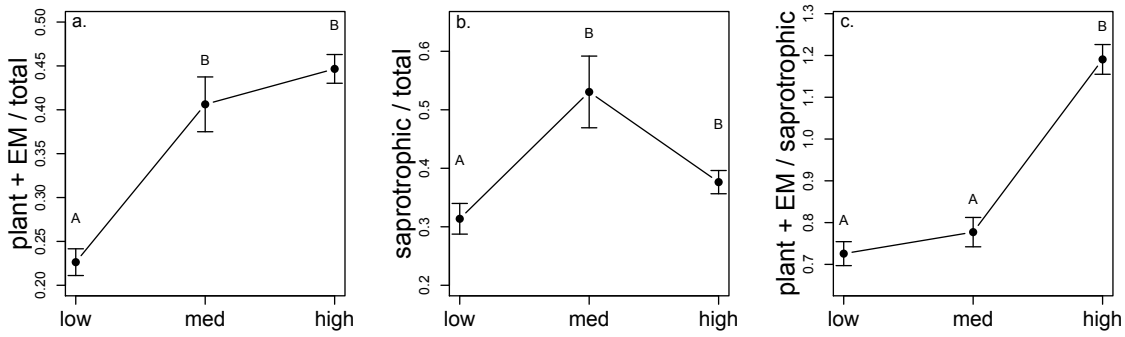

Figure 3.6: Relative fluxes of a) plant + mycorrhizal N uptake to total N decomposition b) saprotrophic microbial N uptake to total N decomposition and c) plant + mycorrhizal N uptake to saprotrophic microbial N uptake. All values are unitless, representing ratios of fluxes in units g N m^{-2} yr^{-1}. Low, medium, and high indicate levels of EM abundance corresponding to young (6 years), intermediate (132 years), and old (200+ years) aged stands. Saprotrophic microbial N uptake includes N uptake by free-living bacteria and fungi.

Chapter 4: Divergence in plant and microbial allocation strategies explains continental patterns in microbial allocation and biogeochemical fluxes[1]

INTRODUCTION

Tradeoffs are pervasive in ecological systems. Organisms must balance multiple objectives with limited resources to maximize growth and fitness (Shoval *et al.* 2012). This is particularly clear when organisms are limited by nutrients, and must split allocation to resource uptake between energy and nutrient acquisition strategies. Ecosystem carbon (C) cycling is inherently sensitive to plant tradeoffs in allocation to roots, which obtain water and nutrients, vs. leaves, the site of C fixation (Franklin *et al.* 2012). Plant root:shoot ratios change continuously as the availability of soil nitrogen (N) or CO_2 in the environment changes, reflecting growth constraints imposed by resource limitation, and a resource acquisition strategy that seeks to balance C vs. N uptake stoichiometry to maximize plant growth. Incorporating this fundamental tradeoff into ecosystem models increases the ability to predict plant productivity and ecosystem C cycling (Dybzinski *et al.* 2011; Franklin *et al.* 2012).

Decomposer microorganisms face a similar allocation tradeoff when investing in C vs. N acquisition. Microorganisms produce different classes of extracellular enzymes to degrade C vs. N-containing organic matter, yielding simple substrates that fuel microbial metabolism and growth. Microbes must allocate limited resources among C-degrading enzymes that target C sources (e.g., cellulose), and N-degrading enzymes that

[1]A version of this chapter has been published. Averill, C. 2014. Divergence in plant and microbial allocation strategies explains continental patterns in microbial allocation and biogeochemical fluxes. *Ecology Letters*, 17: 1202-1210.

target organic nutrients (e.g., protein). Carbon-degrading enzymes are roughly analogous to leaves in plant models, and N-degrading enzymes are analogous to roots. Applying tradeoffs from plant ecology predicts continuous changes in allocation to C vs. N degrading enzymes along gradients of resource availability (Moorhead *et al.* 2012). In support of this, addition of simple nutrients often reduces the production of enzymes that degrade complex forms of the nutrient (Allison & Vitousek 2005). This stoichiometric framework is used to infer microbial C use efficiency from enzyme data, a critical parameter large-scale biogeochemical models (Sinsabaugh & Follstad Shah 2012).

Despite the theoretical grounds for dynamic allocation to different enzymes and resource acquisition strategies by microbes, two common observations suggest that this optimization does not occur:

1. Mineralization of nutrients, converting nutrients from organic to inorganic forms, is a common phenomenon observed in soil microbial communities. Microbes decompose more nutrient-containing organic compounds than needed to meet their stoichiometric demands, and therefore nutrient mineralization occurs in most ecosystems (Schimel & Bennett 2004). Given that soil decomposer microbes have access to very large organic C pools (Allison 2006), the enzymatic resources devoted to 'excess' nutrient acquisition appear to be wasted at the cost of exacerbating C limitation (Moorhead *et al.* 2012).
2. Ratios of C to N enzyme activities are remarkably static in decomposer communities across habitats at global scale (Sinsabaugh *et al.* 2009) suggesting that, for the most part, allocation patterns are not dynamic.

The discrepancy between plant and microbial allocation strategies may be due in part to the fact that organic N sources represent a viable C-acquisition strategy for microbes, but not for plants. Therefore, applying strict tradeoffs between C and N uptake in a microbial allocation model may result in non-optimal allocation strategies. This may generate a fundamentally different optimal allocation pattern for microbial decomposers. Plants can also take up nutrients in organic form, however it likely represents a very small fraction of total plant C uptake (Schimel & Bennett 2004).

Given the importance of plant allocation strategies (Franklin *et al.* 2012) and microbial physiology (Follows *et al.* 2007; Allison *et al.* 2010b; Wieder *et al.* 2013) to understanding ecosystem C fluxes and storage, including microbial allocation strategies in such models may strongly impact predictions of C-cycling rates and storage in soil. To investigate how decomposer microbes should balance allocation to C vs. N decomposition, I created a microbial physiology driven biogeochemical model that prioritizes maximizing carbon acquisition rather than optimizing the stoichiometry of resource uptake (herein referred to as EnzMax). I then compare model behavior to a standard model where allocation is driven solely by optimizing C:N stoichiometry of resource return to match microbial stoichiometry, similar to plant allocation solutions (herein referred to as EnzOpt). To validate these models against empirical data, I compared patterns of enzyme allocation predicted by the two frameworks to a continental data set collected by the National Rivers and Streams Assessment (Hill *et al.* 2012), and examined when these different allocation assumptions generate differences in biogeochemical cycling. By doing so I try to answer two questions:

1. Is there an allocation pattern that maximizes microbial growth while generating static allocation to C vs. N enzymes as nutrient availability changes?
2. What are the biogeochemical consequences of different allocation assumptions in a microbial physiology model?

METHODS

I built a biogeochemical model that seeks to maximize return from enzymatic catalysis of organic matter (hereafter, 'EnzMax') so that resource acquisition and growth of microbial biomass will be greatest under all resource conditions. I then compare this to a model that seeks to acquire resources to match consumer stoichiometric demands, after accounting for consumer C use efficiency (CUE), which I refer to as the optimal stoichiometry model (hereafter, 'EnzOpt'). The EnzOpt model is similar to the Extracellular Enzyme Model (EEZY) created by Moorhead et al. (2012), which represents a microbial foraging strategy that changes continuously as substrate stoichiometry changes. Organisms are constantly trying to match resource uptake to their threshold element ratio, which has been considered to be the best strategy to maximize an organism's biomass growth, and therefore fitness (Sterner & Elser 2002; Allison *et al.* 2010c). The threshold element ratio is the stoichiometric ratio of C to nutrients at which an organism will switch from C to nutrient limitation (Sterner & Elser 2002). Biomass growth is maximized under the EEZY and EnzOpt frameworks when the resource pools matches an organism's threshold element ratio. The primary difference between EnzMax and EnzOpt is that EnzMax will violate the resource acquisition strategy that matches uptake of C and N to the organism's threshold element ratio, if another strategy results in

greater biomass growth. This only occurs if a different allocation pattern generates more C-return per unit time, as well as sufficient N return to utilize the extra C. It is important to note both frameworks have fixed microbial biomass stoichiometry. The C:N ratio of microbial biomass is not allowed to vary. This is a simplifying assumption to make comparisons more tractable.

Both EnzMax and EnzOpt explicitly represent two organic matter resources, C1, a pool of organic matter that contains nutrients (i.e. protein or chitin), and C2, an organic matter pool containing C only (i.e. lignin-cellulose), as well as two enzyme pools, E1 and E2, that specifically target either C1 or C2. Both models assume reaction rates follow reverse Michaelis-Menten enzyme kinetics as implemented in Schimel and Weintraub (2003). This assumes that substrate pool sizes are much larger than enzyme pool sizes, and therefore reaction rates are a saturating function of enzyme, rather than substrate concentration because enzymes compete for binding sites. These conditions are typically met in leaf litter and in many soils, however this may not hold true across all microbial resource environments (Wang & Post 2013). Nevertheless reverse kinetics have proven useful in understanding microbial responses to C and N addition (Schimel and Weintraub 2003), root priming (Drake *et al.* 2013), and changes in microbial community structure (Waring *et al.* 2013). Furthermore, the model can be resolved using forward kinetic assumptions and generate identical allocation predictions, if some simplifying assumptions are made.

In the EEZY model, microbes allocate resources to different enzymes so that the returns match their threshold element ratio, which takes into account both biomass stoichiometry and C lost to respiration during catabolism (i.e., CUE). This is modeled as

$$(1)\ \frac{CN_m}{CUE} = \frac{D_{c1}+D_{c2}}{D_{c1}/CN}$$

CN_m is the C:N ratio of the microbial biomass, CUE is C use efficiency, D_{c1} and D_{c2} are the decomposition rates of C1 and C2, and CN_l is the C:N ratio of the organic nutrient resource (All abbreviations are summarized in Table 1). However, this equation does not account for maintenance respiration costs, which depend on the size of the microbial biomass, and therefore underestimates the microbial threshold element ratio, causing microbes to over-invest in N-degrading enzymes and under invest in C-degrading enzymes in the original EEZY model presented in Moorhead et al (2012). In the EnzOpt model I modify equation 1 to account for maintenance respiration (R_m) costs according to:

$$(1a)\ \frac{CN_m}{CUE} = \frac{D_{c1}+D_{c2}-R_m}{D_{c1}/CN}$$

In equation 1a, D_{c1} and D_{c2} can be replaced by their respective reverse Michaelis-Menten equations, along with the term α that splits the enzyme allocation between E_1 and E_2, which target C1 and C2, respectively. In addition, R_m can be replaced by the microbial biomass size (MBC) times the maintenance respiration parameter (K_m). These replacements result in:

$$(2)\ \frac{CN_m}{CUE} = \frac{\frac{\alpha*k_d*E}{Kes+\alpha*E}+\frac{(1-\alpha)*k_d*E}{Kes+(1-\alpha)*E}-MBC*K_m}{\frac{\alpha*E}{(Kes+\alpha*E)*CN_1}}$$

This equation is then rearranged and solved for α:

$$(3)\ \frac{\mathrm{E}^2*(-\mathrm{MBC})*K_m*CN_1*CUE+2*E^2*CN_1*CUE*K_d-E^2*CN_m*K_d-E*K_{es}*CN_m*K_d+\sqrt{\begin{array}{c}(E^2*MBC*K_m*CN_1*CUE-2*E^2*CN_1*CUE*K_d+E^2*CN_m*K_d+E*K_{es}*CN_m*K_d)^2-\\ 4*\left(E*K_{es}*MBC*K_m*CN_1*CUE-E*K_{es}*CN_1*CUE*K_d+{K_{es}}^2*MBC*K_m*CN_1*CUE\right)*\\ (E^2*(-MBC)*K_m*CN_1*CUE+E^2*CN_1*CUE*K_d-E^2*CN_m*K_d)\end{array}}}{2*(E^2*(-MBC)*K_m*CN_1*CUE+2*E^2*CN_1*CUE*K_d-E^2*CN_m*K_d)}$$

This solution has the advantage of minimizing excess uptake of C or N that cannot be used and must be lost due to overflow mineralization of C or N. Overflow mineralization occurs when microbes do not have enough of the limiting resource (N or C) to match C or N uptake. An analogous type of decision statement for a plant model would cause plants to decrease root allocation and increase shoot allocation as soil nutrients increase.

The stoichiometric solution makes sense when microbes are nutrient limited, because it maximizes nutrient return while balancing stoichiometric requirements. However, when microbes are C-limited they should adjust enzyme allocation to optimize C return and maximize growth, rather than to balance microbial stoichiometry. Total C decomposition can be represented as the sum of decomposition of C1 and C2 resources:

$$(4)\ D_{Ctot} = D_{c1} + D_{c2}$$

This equation is then rewritten replacing D_{C1} and D_{C2} terms with their respective reverse Michaelis-Menten equations:

$$(5)\ D_{Ctot} = \frac{\alpha*k_d*E}{K_{es}+\alpha*E} + \frac{(1-\alpha)*k_d*E}{K_{es}+(1-\alpha)*E}$$

D_{Ctot} can be maximized by taking the derivative of D_{Ctot} with respect to α ($\partial D_{Ctot}/\partial\alpha$), setting $\partial D_{Ctot}/\partial\alpha$ to 0, and solving for α.

$$(6)\ \frac{\partial D_{Ctot}}{\partial \alpha} = \frac{k_d * E^2 * K_{es} * (2\alpha - 1) * (E + 2K_{es})}{(E * (-\alpha) + E + K_{es})^2 * (E * \alpha + K_{es})^2}$$

When solved for $\partial D_{Ctot}/\partial \alpha = 0$, $\alpha = 0.5$ so long as E and K_{es} are never both zero. K_{es} cannot be zero. Hence, allocation to C vs. nutrient degrading enzymes should be 1:1 to maximize C return when microbes are C-limited, given the other assumptions of this model structure.

I implemented this decision statement into the EnzMax model. When microbial biomass is C limited, $\alpha = 0.5$, as this maximizes microbial biomass. When microbial biomass is nutrient limited α is calculated according to equation 3, which seeks to satisfy stoichiometric balance. Nutrient limitation is determined as it is in Schimel and Weintraub (2003); after producing enzymes, microbes are nutrient limited if they do not take up enough N to grow after satisfying N requirements of enzyme production, C costs of respiration associated with enzyme production, and maintenance respiration. A simple schematic of the model highlighting allocation to difference enzymes can be seen in Figure 4.1.

The second modification I made to the EEZY model structure is to track two explicit enzyme pools. The original EEZY model structure had one enzyme pool, and relative enzymes pools are calculated by multiplying the single enzyme pool by the α parameter. This works well in EEZY as alpha changes continuously. In EnzMax, α toggles between 0.5 and the nutrient limitation calculation at intermediate CN ratios as microbes position themselves at the edge of C and nutrient limitation. This can generate wild swings in the abundance of the E1 and E2 pools. To minimize this, the α statement

now only modifies enzyme production; thus, microbes can adjust which enzyme is produced each time step, but cannot convert E1 into E2 based on nutrient limitation. This modification is technical, and not a major change in model structure.

Co-option of soil extracellular enzymes by 'cheating' microbes can alter the return on investment of enzyme production and negatively affect microbial population size (Gore et al. 2009). Inclusion of cheating processes into the model was considered, as it would affect the effective enzyme turnover rate. However, this modification should not change predicted allocation patterns, so long as cheating microbes are just as likely to co-opt C enzymes as they are N enzymes. This is because I assume the same co-option rate for both classes of enzymes, and the turnover rate does not enter either allocation function. As long as beggars cannot be choosers, cheaters are not actively choosing which products they steal, and neither product (C- or N-degrading enzyme) is more likely to go to the cheaters than the other, the allocation decisions should remain the same.

Model simulations: I ran both the EnzOpt and EnzMax models over a C:N range of 5-50, by manipulating the CN ratio of the nutrient containing pool from 2.5-25. This range of CN was chosen in order to be comparable to the results of Moorhead et al. (2012). The CN ratio is determined by summing the C pools and dividing by the N pool of C1. In effect this model structure can only change nutrient availability by altering the CN ratio of the C1 pool. The CN ratio of the entire soil C pool can also be altered by increasing or decreasing the abundance of C2 relative to C1, however this has no effect on nutrient availability to decomposers in this model structure. This discrepancy will make it more challenging to validate results with empirical data, as the assumption that

C2 ~ C1 may not always hold. However, so long as the central limit theorem holds, sufficient sample size should be able to overcome this problem and test which model predictions (EnzMax or EnzOpt) hold up against field data.

Because the EnzMax results in stable oscillations at some CN ratios at equilibrium, I averaged model outputs over 200 days, after the model had reached equilibrium. All model simulations were run using R statistical software (R Core Team 2014).

Testing model with empirical data: I tested model predictions using data collected for the National Rivers and Streams Assessment by the United States Environmental Protection Agency (Hill *et al.* 2012). The data set includes measurements of stream sediment potential enzyme activity paired with total sediment C and N observations. Although the EnzMax model was developed based on theory derived from soil decomposer systems, previous work has found controls of enzyme activities in stream and river sediments to be similar to those found in soils (Arnosti *et al.* 2014). Furthermore, stoichiometric and growth efficiency theories developed for soil microbes have been successfully applied to stream sediment microbial communities (Sinsabaugh *et al.* 2012). The EnzMax model makes predictions regarding the production and abundance of C and N degrading enzymes, and their relative abundances. The data set is therefore appropriate to test the prediction of EnzMax, so long as potential enzyme activities are indicative of overall enzyme concentrations (Wallenstein & Weintraub 2008). I summed across all hydrolytic C-degrading and N-degrading enzymes that were measured, only including records that had complete data for all enzymes. Enzymes were summed to

determine total investment in C and N degrading enzymes classes, rather than focusing on subsets. C enzymes measured included alpha-galactosidase, beta-galactosidase, alpha-glucosidase, beta-glucosidase, and xylosidase. N-degrading enzymes included leucine amino-peptidase, alanine amino-peptidase and N-acetyl-glucosaminidase. C:N ratios were calculated by dividing total sediment C by total sediment N. I averaged across multiple measurements within sites, as well as multiple observation time points within sites. I excluded 10 observations that had unusually high sediment C:N ratios (> 100) as well as urban streams, yielding 651 unique observations for analysis. All enzyme data were natural log transformed to improve the normality of residuals and satisfy homoscedasticity (Sinsabaugh *et al.* 2009). I modeled C-enzymes as a function N enzymes and sediment C:N ratio, and then tested for a breakpoint in the relationship between C enzymes and sediment C:N in the full model using a one-tailed Davies-test implemented using the segmented package for R-statistical software (Muggeo 2003, 2008). My expectation, based on model simulations, was that there would be no relationship before the threshold and a negative relationship after the threshold. I plot both the observed vs. predicted values of the full statistical model, as well as the breakpoint relationship between sediment C:N and C-enzyme model residuals after the relationship between C and N-enzymes has been accounted for based on parameter estimates of the full segmented model. This plot details the variation in C vs. N enzyme concentrations that is not accounted for by their own inherent correlation with each other. Values near 0 indicate near 1:1 potential enzyme activity, while values below 0 represent increasing allocation to N-degrading enzymes.

RESULTS

In EnzMax the mathematical solution to optimize microbial growth under C-limitation is equal allocation (or 1:1 allocation) to C vs. N-acquiring enzymes. This allocation pattern does not change across substrate C:N ratios of 5-20, at which point there is a threshold in allocation, and microbes begin increasing allocation to N-degrading enzymes. Declining returns on investment in either resource acquisition strategy drive this result, making equal allocation to each strategy intuitive when microbes are C-limited. In contrast to EnzMax, EnzOpt predicts continuous changes in allocation to C vs. N-degrading enzymes across all C:N ratios, similar to allocation patterns in plant models (Franklin *et al.* 2012). Once microbial nutrient limitation occurs, EnzMax and EnzOpt converge on nearly identical allocation patterns (Figure 4.2).

Importantly, the static allocation strategy in EnzMax that emerged from the EnzMax solution outperforms the dynamic EnzOpt strategy in terms of total microbial biomass in the system by up to ~60% when microbes are under conditions of C-limitation (Figure 4.3a). Under reverse Michaelis-Menten enzyme kinetics, increasing investment in an enzyme always results in diminishing C return over time as enzymes saturate the substrate surface. Thus, the best solution under C-limitation is to allocate equally to the two enzymes, thereby optimizing C return for both. This 1:1 allocation strategy causes greater total respiration and soil C loss in EnzMax as compared to the EnzOpt model (Figure 4.3b).

At C:N ratios below 20 EnzMax and EnzOpt diverged substantially in terms of microbial biomass C, N mineralization, overflow and total respiration (Figure 4.4a,

Figure 4.4b). The EnzOpt and EnzMax models showed nearly identical biogeochemical patterns at C:N ratios greater than ~20 when their allocation strategies converged. Importantly, EnzMax predicts N mineralization at some C:N ratios, while EnzOpt cannot.

The full statistical model explained 78% of the variation in the National Rivers and Streams Assessment data set (Figure 4.5a). Furthermore, breakpoint analysis on the full model revealed a significant breakpoint in the relationship between C vs. N-enzyme allocation and sediment C:N ratio at a sediment C:N value of 18.3 (± 2.7 s.e., $P = 0.001$, Figure 4.5b). This overlaps with the predicted breakpoint based on the EnzMax model. Before this breakpoint allocation is static (the slope is not significantly different from 0), and afterwards the stoichiometry of C vs. N enzymes declines, indicating increased allocation to N-degrading enzymes as N becomes more limiting. This behavior is consistent with the EnzMax, but not the EnzOpt allocation framework.

DISCUSSION

By changing how C:N stoichiometry is integrated in microbial decomposition models, EnzMax can resolve the apparent contradiction between 1:1 enzyme allocation at global scales and other evidence for shifts in microbial allocation with C or N additions. Static allocation to C vs. N acquisition enzymes over a wide range of nutrient availability was the best allocation strategy to maximize microbial biomass growth, and could not be predicted by the EnzOpt model that prioritizes stoichiometric constraints when making allocation decisions. Dynamic allocation was only optimal above a certain threshold substrate C:N ratio (~20) where microbes must invest more in nutrient acquisition to maximize biomass and growth. This contrasts with most other allocation tradeoffs in

ecology that are dynamic as resource availability changes (MacArthur & Pianka 1966; Franklin *et al.* 2012). The key difference is that organic nutrients represent both a C-resource and a nutrient resource. Diminishing returns on enzyme investment favor equal allocation to each type of enzyme, optimizing C returns to the enzyme producer. This provides a theoretical grounding to relatively static enzyme ratios observed across the globe (Sinsabaugh *et al.* 2009) and is supported by the analysis of enzyme ratios in this paper. 1:1 allocation to C and nutrient acquisition strategies challenges previous estimates of microbial CUE based on enzyme ratios and stoichiometric allocation assumptions, and represents a departure between micro and macro ecology.

Behavior of EnzMax vs. EnzOpt models: The largest differences between the EnzMax and EnzOpt models are under conditions of C-limitation. EnzMax outperformed EnzOpt, with large increases in microbial biomass growth, and C and N mineralization because microbes in EnzMax view organic N substrates as primarily a C-resource, rather than a nutrient containing organic compound. EnzMax therefore divides investment in C-only and C+N organic substrate decomposition equally, due to declining returns on investment from individual enzymes. By contrast, the EnzOpt model seeks to tune return from enzyme catalysis to microbial stoichiometry, and therefore over-invests in C-only compounds and under-invests in organic N containing compounds at low C:N.

This difference in model behavior has three important consequences for microbial ecology. First, microbial growth and total microbial biomass should be maximized on all substrates before N-availability begins to limit microbial growth. In contrast, past microbial allocation models predicted optimal growth at a single substrate C:N, where

substrate stoichiometry matches consumer stoichiometry, consistent with the idea of a threshold element ratio (Sterner & Elser 2002; Sinsabaugh *et al.* 2009; Moorhead *et al.* 2012). Second, the EnzMax allocation strategy provides a mechanistic foundation for why microbes should mineralize N, because decomposition of N is no longer coupled to microbial growth. An optimal stoichiometry model cannot predict N mineralization. Finally, this allocation strategy predicts static allocation to C vs. N targeting enzymes over a broad range of substrate C:N ratios before N-limitation, rather than dynamic shifts in allocation along gradients of substrate stoichiometry as observed in plant communities (Dybzinski *et al.* 2011), and consistent with global analysis of decomposer enzyme stoichiometry (Sinsabaugh *et al.* 2009). As we move to integrate microbial physiology models into coupled C and N models of ecosystems and Earth climate, microbial allocation strategies will be central in determining the magnitude of microbial fluxes of N and CO_2.

Model Predictions vs. Empirical data: A major prediction of EnzMax is that the ratio of C:N degrading enzymes should be constant with respect to substrate C:N, up to a critical threshold, at which point they should decline as microbes increase investment in organic N degrading enzymes. The analysis of the National Rivers and Streams Assessment data supports this prediction at a sediment C:N threshold of 18.3 and the observed standard deviation overlaps the predicted value of EnzMax. Further support for EnzMax comes from relatively static enzyme ratios across the globe (Sinsabaugh *et al.* 2009). Although my analysis shows that enzyme C:N ratios do deviate after a threshold, 410 of 651 total observations (63%) in the analysis fall on the static side of the

breakpoint, resulting in a mean enzyme ratio of 0.92 (± 0.51 SD), and strong correlation between the activity of C and N degrading enzymes. Relatively static global enzyme ratios may therefore reflect C-limitation in most microbial ecosystems, rather than stoichiometric matching between microbial communities and their resource environments.

The effect of experimental manipulations of C and N availability are also consistent with the EnzMax framework. Addition of organic N compounds to soils does not generate an increase in production of N-degrading enzymes unless it has been added in combination with labile organic C, thereby relieving C-limitation and inducing N-limitation (Allison & Vitousek 2005). For example, inorganic N addition in boreal forests soils, which are characteristically N limited, causes a decline in N-degrading enzymes and increases in C-degrading enzymes (Allison *et al.* 2010a). More generally, in many studies, N additions have had either negative or neutral total effects on N-degrading enzyme activity (Sinsabaugh & Follstad Shah 2012). The EnzMax framework may explain this in part, because the production of N-degrading enzymes is likely linked to C availability, rather than N-acquisition in many C-limited microbial ecosystems.

EnzMax assumes complex resources are abundant compared to microbial biomass, a condition that is likely met in soils and sediments (Allison 2006), however the stoichiometric predictions may fail in low resource environments. Furthermore, predictions may not extend as easily to phosphorus degrading enzymes, which often cleave phosphate groups from organic compounds, allowing microbes to degrade and take up phosphate without the associated C. This would violate the assumption of

EnzMax that the decomposition products of nutrient degrading enzymes are organic nutrients. Despite these limitations, the modeling and analysis presented here refines understanding of our core assumptions, and builds a framework in which to test the importance of these potential shortcomings.

A final potential shortcoming is the use of a reverse kinetic assumption to represent decomposition fluxes. However, the model can be resolved using forward kinetics and show the predictions are similar under C-limitation, if some assumptions are made regarding the size of the organic matter pool relative to K_m values. If substrate concentrations are low relative to K_m, then relative substrate concentrations will drive allocation decisions before N-limitation. Substrate concentration dependent allocation has been observed using substrates that represent a small fraction of the organic matter pool, but no concentration sensitivity has been detected among substrates that are dominant in the organic matter pool (German *et al.* 2011). Furthermore, if the relative concentration of substrates was driving allocation to C vs N degrading enzymes, then we would predict an increase in allocation to N-degrading enzymes at very low C:N values to maximize C and N acquisition, however this is not observed in the empirical data (Figure 4.5).

Biogeochemical Insights from EnzMax: Coupled C and N cycles are necessary to understand ecosystem level changes in biogeochemical cycles (Finzi *et al.* 2011) and substantially alter Earth climate predictions (Bonan & Levis 2010). Microbial explicit frameworks have tremendous potential to improve our understanding of large-scale biogeochemical processes (Todd-Brown *et al.* 2012; Treseder *et al.* 2012). Enzyme-driven microbial physiology models have become the forefront in predicting soil C

responses to environmental change (Allison *et al.* 2010b; Davidson *et al.* 2012; Wieder *et al.* 2013). These models do a much better job predicting global soil C distributions than past phenomenological models, and substantially alter global climate predictions in Earth simulation models (Wieder *et al.* 2013). As we move to merge microbial physiology models with existing ecosystem models, representing tradeoffs between microbial C and N acquisition will likely be important in capturing the respective processes, just as plant physiological models that include resource allocation tradeoffs between roots and shoots have improved ecosystem C-cycling models (Franklin *et al.* 2012). EnzMax predicts much greater C and N mineralization than a stoichiometric optimization model over a broad range of common soil and sediment C:N ratios. Incorporating the EnzMax resource allocation strategy into a biogeochemical model would dramatically alter the predictions of soil C loss via respiration, and N-mineralization, which is closely associated with NPP and therefore C-inputs to the ecosystem (Reich *et al.* 1997).

Furthermore, The results of EnzMax imply that microbial growth efficiencies may be decoupled from ratios of potential enzyme activities under some conditions. Many biogeochemical equilibrium models assume microbes produce enzymes to match resource return with microbial stoichiometry (Sinsabaugh & Follstad Shah 2012). EnzMax shows that under conditions of C-limitation this assumption is violated, and therefore enzyme ratios cannot be used to infer threshold element ratios, element assimilation efficiencies, or microbial growth efficiency.

A potential shortcoming of EnzMax is that it always predicts N addition will either increase microbial activity and result in net soil C loss, or will not affect microbial

activity, as microbes will be C- rather than N-limited. The empirical evidence for this prediction is mixed, with increased microbial activity and C loss in some N-addition experiments in markedly N-limited systems (Mack *et al.* 2004; Allison *et al.* 2010a) and decreased microbial activity and increased C storage in others (Waldrop *et al.* 2004; Pregitzer *et al.* 2007). Based on the EnzMax model, N addition may not always change soil C cycling but would be unlikely to increase soil C storage. However, microbial physiology is likely to be more complex than modeled here. For example, additions of nutrients may simultaneously alter microbial CUE, leading to enhanced C-storage despite no change in enzyme allocation (Cotrufo *et al.* 2013). Furthermore, other parameters that have been implemented as constants in microbial physiology models (including this one) may indeed be tradeoffs themselves that are affected by nutrient availability, such as total allocation to production of extracellular enzymes (Steinweg *et al.* 2013). Shifts in enzyme production may also reflect changes in community composition, rather than changes in allocation per se (sensu Follows *et al.* 2007). Finally, N addition often reduces plant allocation belowground (Franklin *et al.* 2012), which may be subsidizing a large fraction of microbial decomposition via root exudation and allocation to mycorrhizal fungi (Phillips *et al.* 2011).

The response of decomposer microbes to environmental change is complex and driven by a nuanced physiology and interactions with primary producers. Refining our mechanistic understanding of the physiology and ecology of these organisms will improve our ability to make accurate predictions of ecosystem response to environmental change. EnzMax achieves this by uncovering an optimal strategy for enzyme allocation

in microbial systems. It represents a departure from stoichiometric thinking developed for plant systems, which assume organisms allocate to resource acquisition strategies to match the organisms' stoichiometric demand. Because nutrients are organic in decomposer ecosystems this assumption is violated, resulting in a static allocation strategy across gradients in C vs. N availability up to a threshold. The departures between EnzMax and stoichiometric optimization models of C and N cycling imply that including microbial tradeoffs in resource acquisition will be necessary to capture C and N dynamics and therefore ecosystem C balance in future ecosystem and Earth C models.

CN_m	Microbial biomass C:N stoichiometry
CUE	Microbial carbon use efficiency
Dc_1	Decomposition of carbon pool 1
Dc_2	Decomposition of carbon pool 2
CN_1	CN ratio of carbon pool 1
R_m	Maintenance respiration flux
α	Fraction of enzyme production allocated to enzyme 1
E	Total enzyme C pool
K_{es}	Half saturation constant of enzymes on substrates
MBC	Microbial biomass carbon pool
K_m	Maintenance respiration coefficient
D_{Ctot}	Total decomposition of carbon

Table 4.1: Model parameter, pool and flux abbreviations.

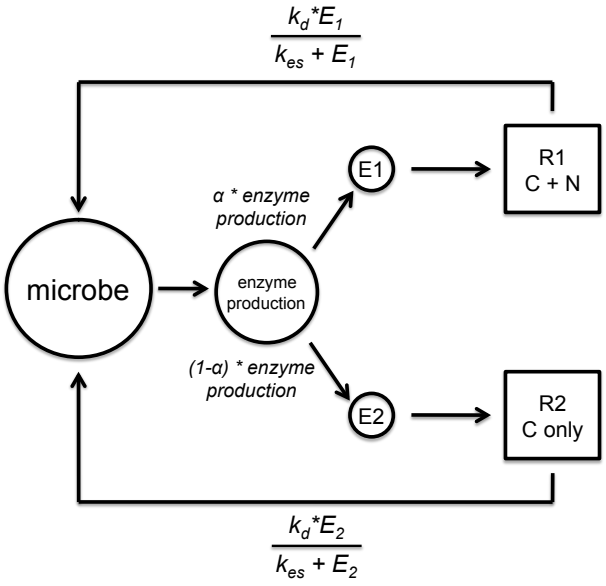

Figure 4.1: Model schematic highlighting how enzyme production is split between the two enzyme pools, and how resource fluxes returned to microbes are calculated. The alpha parameter splits enzyme production between enzyme 1 and enzyme 2 pools.

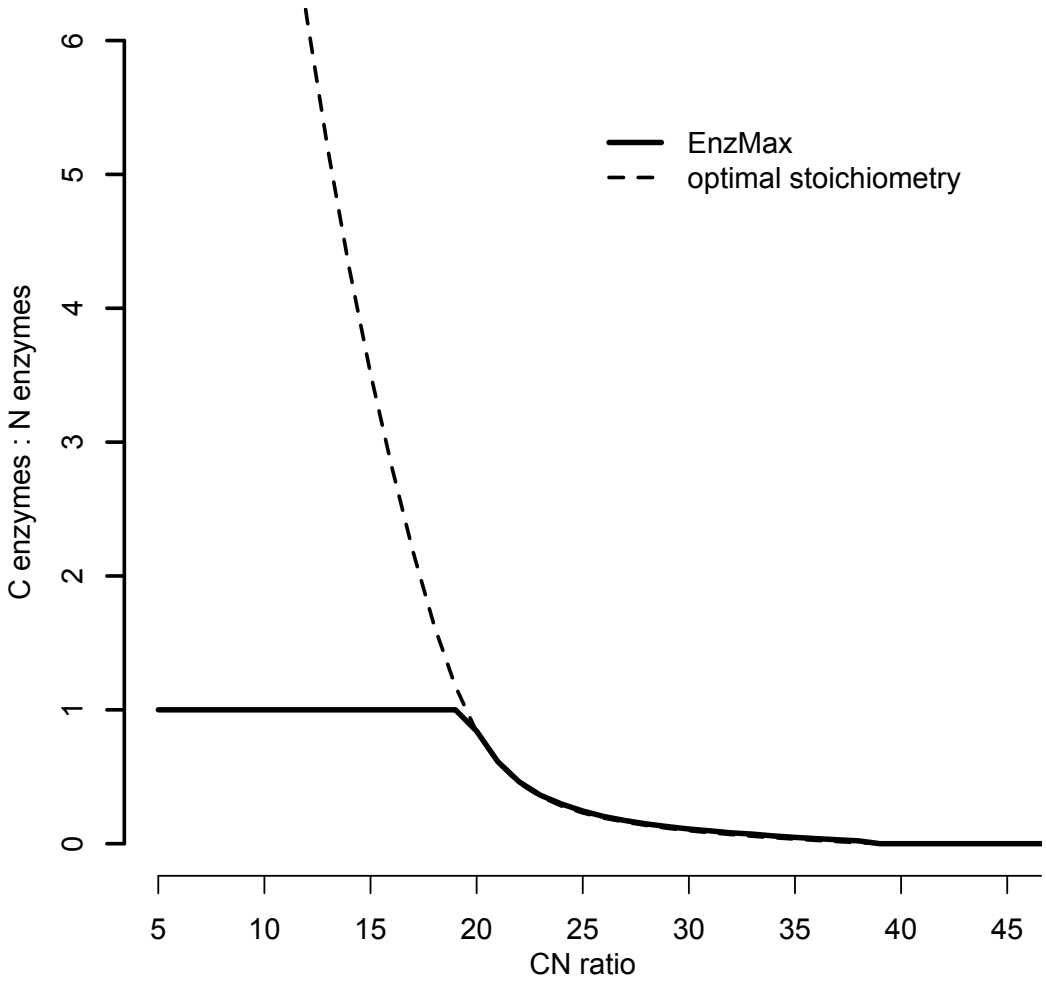

Figure 4.2: Ratio of C enzymes to N enzymes in EnzMax and EnzOpt models as they change along a gradient of substrate C:N.

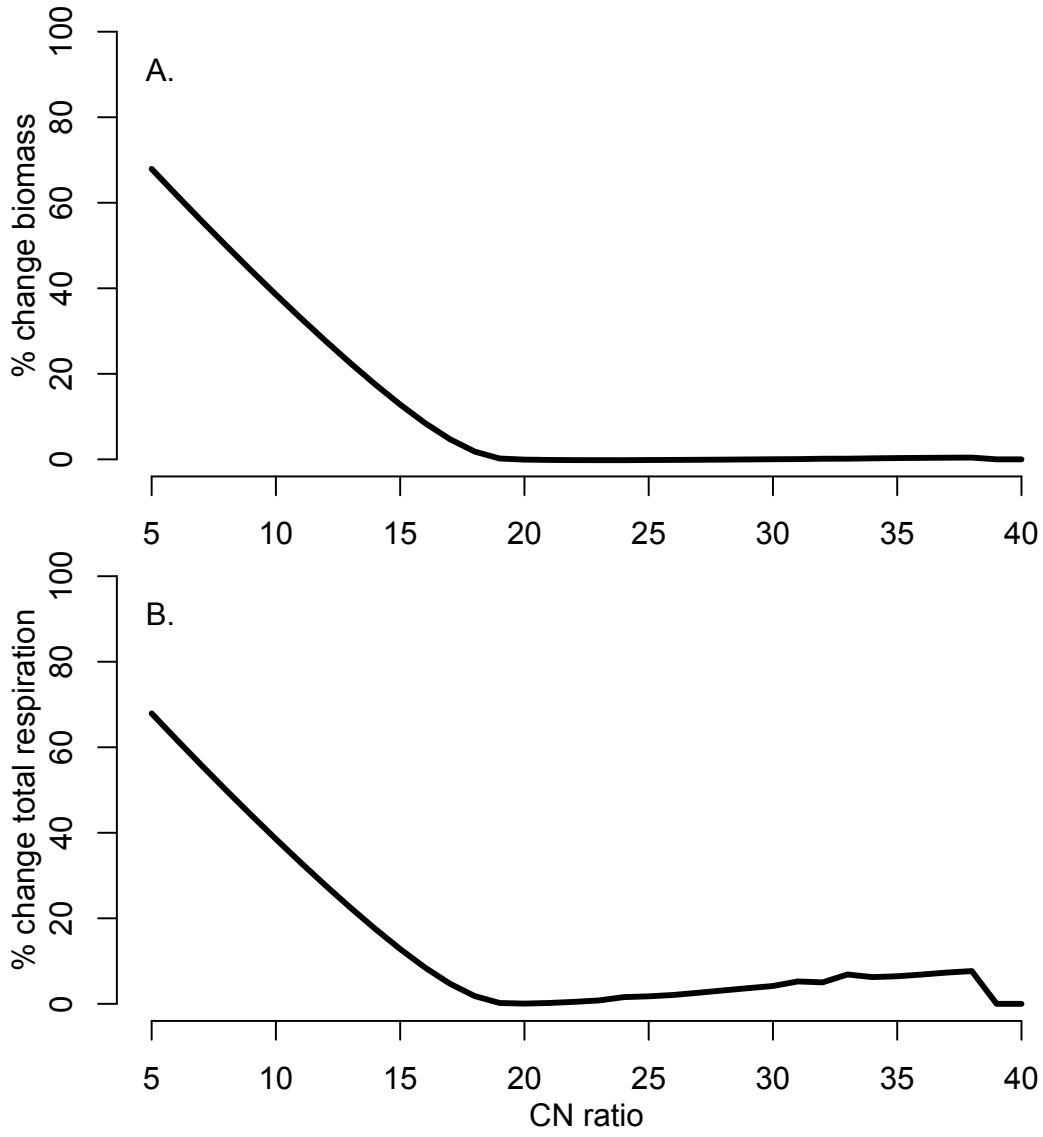

Figure 4.3: Difference in A. microbial biomass and B. total respiration of EnzMax model outputs shown as a percentage difference from EnzOpt outputs.

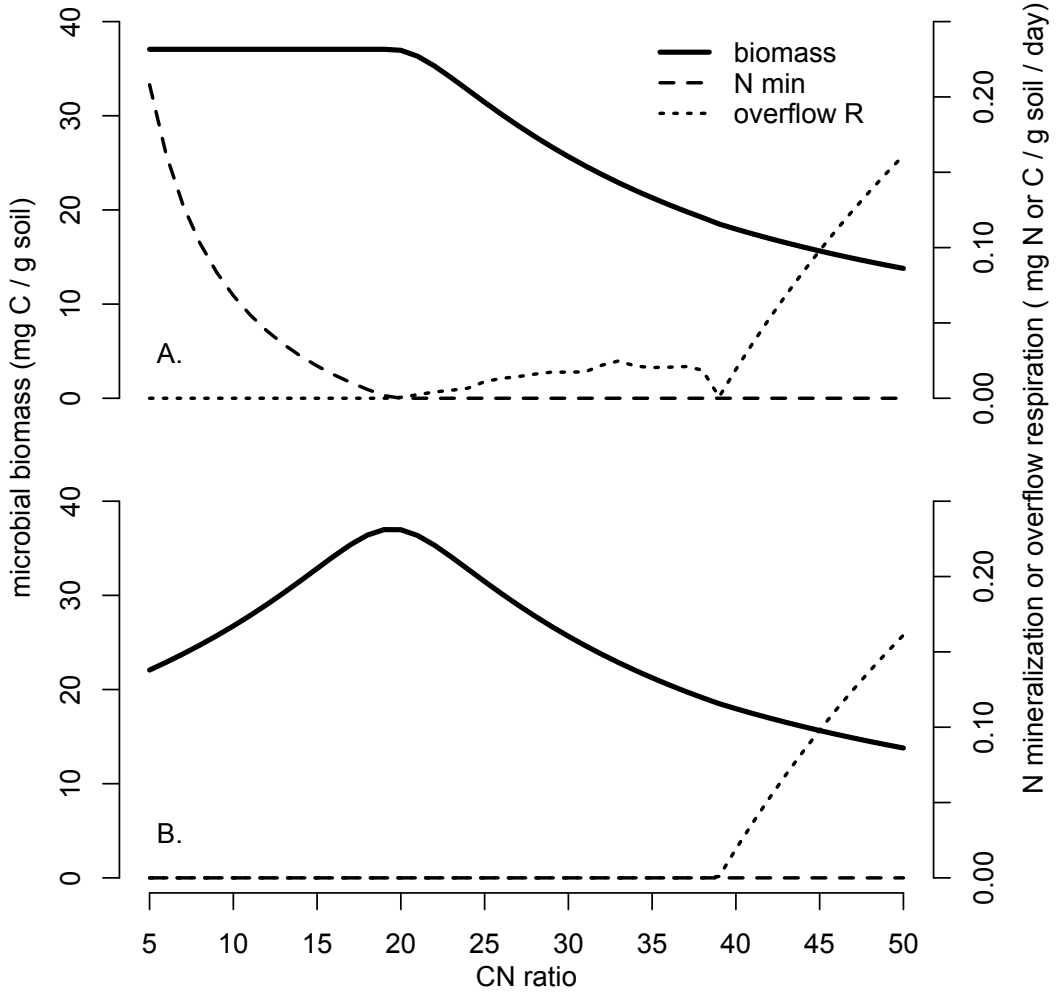

Figure 4.4: Behavior of A. EnzMax and B. EnzOpt models vs. substrate C:N. Microbial biomass is plotted against the left y-axis. N mineralization and overflow respiration are plotted against the right y-axis.

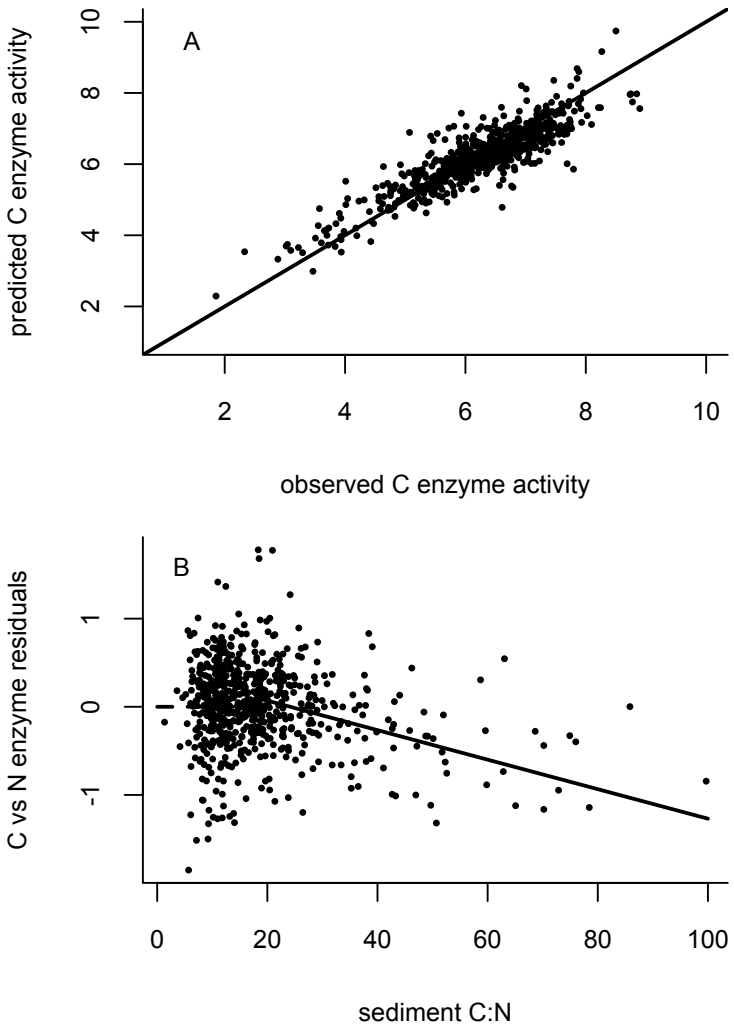

Figure 4.5: (A) Observed vs. predicted values of the full model (carbon enzyme concentration as a function of nitrogen enzyme concentration and sediment C:N, both enzyme parameters were natural log transformed, total model R2=0.78). (B) Relationship between the C-enzyme concentration residuals and sediment C:N after accounting for the relationship with N-enzyme concentrations. Both C and N enzyme concentrations are natural log transformed. A dashed line with a slope of 0 before the breakpoint is shown for visualization, there is no significant relationship before the breakpoint.

References

Allison, S. D. 2006. Brown ground: a soil carbon analogue for the green world hypothesis? The American Naturalist 167:619–627.

Allison, S. D., T. B. Gartner, M. C. Mack, K. McGuire, and K. Treseder. 2010a. Nitrogen alters carbon dynamics during early succession in boreal forest. Soil Biology and Biochemistry 42:1157–1164.

Allison, S. D., and P. M. Vitousek. 2005. Responses of extracellular enzymes to simple and complex nutrient inputs. Soil Biology and Biochemistry 37:937–944.

Allison, S. D., M. D. Wallenstein, and M. A. Bradford. 2010b. Soil-carbon response to warming dependent on microbial physiology. Nature Geoscience 3:336–340.

Allison, S. D., M. N. Weintraub, T. B. Gartner, and M. P. Waldrop. 2010c. Evolutionary-Economic Principles as Regulators of Soil Enzyme Production and Ecosystem Function. Pages 229–243 *in* G. Shukla and A. Varma, editors. Soil Enzymology. Springer Berlin Heidelberg, Berlin, Heidelberg.

Arnosti, C., C. Bell, D. L. Moorhead, R. L. Sinsabaugh, A. D. Steen, M. Stromberger, M. Wallenstein, and M. N. Weintraub. 2014. Extracellular enzymes in terrestrial, freshwater, and marine environments: perspectives on system variability and common research needs. Biogeochemistry 117:5–21.

Averill, C. 2014. Divergence in plant and microbial allocation strategies explains continental patterns in microbial allocation and biogeochemical fluxes. Ecology Letters 17:1202–1210.

Averill, C., B. L. Turner, and A. C. Finzi. 2014. Mycorrhiza-mediated competition between plants and decomposers drives soil carbon storage. Nature 505:543–545.

Bödeker, I. T. M., K. E. Clemmensen, W. de Boer, F. Martin, Å. Olson, and B. D. Lindahl. 2014. Ectomycorrhizal *Cortinarius* species participate in enzymatic oxidation of humus in northern forest ecosystems. New Phytologist 203:245–256.

Bonan, G. B., and S. Levis. 2010. Quantifying carbon-nitrogen feedbacks in the Community Land Model (CLM4): CARBON-NITROGEN FEEDBACKS IN CLM4. Geophysical Research Letters 37:n/a–n/a.

Bradford, M. A., C. A. Davies, S. D. Frey, T. R. Maddox, J. M. Melillo, J. E. Mohan, J. F. Reynolds, K. K. Treseder, and M. D. Wallenstein. 2008. Thermal adaptation of soil microbial respiration to elevated temperature. Ecology Letters 11:1316–1327.

Brzostek, E. R., D. Dragoni, Z. A. Brown, and R. P. Phillips. 2015. Mycorrhizal type determines the magnitude and direction of root-induced changes in decomposition in a temperate forest. New Phytologist:n/a–n/a.

Brzostek, E. R., and A. C. Finzi. 2011. Substrate supply, fine roots, and temperature control proteolytic enzyme activity in temperate forest soils. Ecology 92:892–902.

Caporaso, J. G., J. Kuczynski, J. Stombaugh, K. Bittinger, F. D. Bushman, E. K. Costello, N. Fierer, A. G. Peña, J. K. Goodrich, J. I. Gordon, G. A. Huttley, S. T. Kelley, D. Knights, J. E. Koenig, R. E. Ley, C. A. Lozupone, D. McDonald, B. D. Muegge, M. Pirrung, J. Reeder, J. R. Sevinsky, P. J. Turnbaugh, W. A. Walters, J. Widmann, T. Yatsunenko, J. Zaneveld, and R. Knight. 2010. QIIME allows

analysis of high-throughput community sequencing data. Nature Methods 7:335–336.
Cheng, L., F. L. Booker, C. Tu, K. O. Burkey, L. Zhou, H. D. Shew, T. W. Rufty, and S. Hu. 2012. Arbuscular Mycorrhizal Fungi Increase Organic Carbon Decomposition Under Elevated CO2. Science 337:1084–1087.
Clemmensen, K. E., A. Bahr, O. Ovaskainen, A. Dahlberg, A. Ekblad, H. Wallander, J. Stenlid, R. D. Finlay, D. A. Wardle, and B. D. Lindahl. 2013. Roots and Associated Fungi Drive Long-Term Carbon Sequestration in Boreal Forest. Science 339:1615–1618.
Clemmensen, K. E., A. Michelsen, S. Jonasson, and G. R. Shaver. 2006. Increased ectomycorrhizal fungal abundance after long-term fertilization and warming of two arctic tundra ecosystems. New Phytologist 171:391–404.
Cotrufo, M. F., M. D. Wallenstein, C. M. Boot, K. Denef, and E. Paul. 2013. The Microbial Efficiency-Matrix Stabilization (MEMS) framework integrates plant litter decomposition with soil organic matter stabilization: do labile plant inputs form stable soil organic matter? Global Change Biology 19:988–995.
Davidson, E. A., S. Samanta, S. S. Caramori, and K. Savage. 2012. The Dual Arrhenius and Michaelis-Menten kinetics model for decomposition of soil organic matter at hourly to seasonal time scales. Global Change Biology 18:371–384.
Doane, T. A., and W. R. Horwath. 2003. Spectrophotometric Determination of Nitrate with a Single Reagent. Analytical Letters 36:2713–2722.
Drake, J. E., B. A. Darby, M.-A. Giasson, M. A. Kramer, R. P. Phillips, and A. C. Finzi. 2013. Stoichiometry constrains microbial response to root exudation- insights from a model and a field experiment in a temperate forest. Biogeosciences 10:821–838.
Drake, J. E., A. Gallet-Budynek, K. S. Hofmockel, E. S. Bernhardt, S. A. Billings, R. B. Jackson, K. S. Johnsen, J. Lichter, H. R. McCarthy, M. L. McCormack, D. J. P. Moore, R. Oren, S. Palmroth, R. P. Phillips, J. S. Pippen, S. G. Pritchard, K. K. Treseder, W. H. Schlesinger, E. H. DeLucia, and A. C. Finzi. 2011. Increases in the flux of carbon belowground stimulate nitrogen uptake and sustain the long-term enhancement of forest productivity under elevated CO2: C fluxes belowground and long-term FACE productivity. Ecology Letters 14:349–357.
Dybzinski, R., C. Farrior, A. Wolf, P. B. Reich, and S. W. Pacala. 2011. Evolutionarily Stable Strategy Carbon Allocation to Foliage, Wood, and Fine Roots in Trees Competing for Light and Nitrogen: An Analytically Tractable, Individual-Based Model and Quantitative Comparisons to Data. The American Naturalist 177:153–166.
Edgar, R. C. 2010. Search and clustering orders of magnitude faster than BLAST. Bioinformatics 26:2460–2461.
Feng, Z., T. Rütting, H. Pleijel, G. Wallin, P. B. Reich, C. I. Kammann, P. C. D. Newton, K. Kobayashi, Y. Luo, and J. Uddling. 2015. Constraints to Nitrogen Acquisition of Terrestrial Plants under Elevated CO_2. Global Change Biology:n/a–n/a.

Fierer, N., J. A. Jackson, R. Vilgalys, and R. B. Jackson. 2005. Assessment of Soil Microbial Community Structure by Use of Taxon-Specific Quantitative PCR Assays. Applied and Environmental Microbiology 71:4117–4120.

Fierer, N., M. S. Strickland, D. Liptzin, M. A. Bradford, and C. C. Cleveland. 2009. Global patterns in belowground communities. Ecology Letters 12:1238–1249.

Finzi, A. C., J. J. Cole, S. C. Doney, E. A. Holland, and R. B. Jackson. 2011. Research frontiers in the analysis of coupled biogeochemical cycles. Frontiers in Ecology and the Environment 9:74–80.

Finzi, A. C., R. J. Norby, C. Calfapietra, A. Gallet-Budynek, B. Gielen, W. E. Holmes, M. R. Hoosbeek, C. M. Iversen, R. B. Jackson, M. E. Kubiske, and others. 2007. Increases in nitrogen uptake rather than nitrogen-use efficiency support higher rates of temperate forest productivity under elevated CO2. Proceedings of the National Academy of Sciences 104:14014–14019.

Finzi, A. C., P. C. L. Raymer, M. A. Giasson, and D. A. Orwig. 2014. Net primary production and soil respiration in New England hemlock forests affected by the hemlock woolly adelgid. Ecosphere 5:art98.

Follows, M. J., S. Dutkiewicz, S. Grant, and S. W. Chisholm. 2007. Emergent Biogeography of Microbial Communities in a Model Ocean. Science 315:1843–1846.

Franklin, O., J. Johansson, R. C. Dewar, U. Dieckmann, R. E. McMurtrie, A. Brannstrom, and R. Dybzinski. 2012. Modeling carbon allocation in trees: a search for principles. Tree Physiology 32:648–666.

Friedel, J. K., and E. Scheller. 2002. Composition of hydrolysable amino acids in soil organic matter and soil microbial biomass. Soil Biology and Biochemistry 34:315–325.

Gadgil, R. L., and P. D. Gadgil. 1971. Mycorrhiza and Litter Decomposition. Nature 233:133–133.

Gadgil, R. L., and P. D. Gadgil. 1975. Suppression of litter decomposition by mycorrhizal roots if *Pinus radiata*. New Zealand Journal of Forest Science 5:33–41.

Garcia, M. O., T. Ovasapyan, M. Greas, and K. K. Treseder. 2008. Mycorrhizal dynamics under elevated CO2 and nitrogen fertilization in a warm temperate forest. Plant and Soil 303:301–310.

Gardes, M., and T. D. Bruns. 1993. ITS primers with enhanced specificity for basidiomycetes - application to the identification of mycorrhizae and rusts. Molecular Ecology 2:113–118.

Gelman, A., and J. Hill. 2007. Data analysis using regression and multilevel/hierarchical models. Cambridge University Press, Cambridge ; New York.

German, D. P., S. S. Chacon, and S. D. Allison. 2011a. Substrate concentration and enzyme allocation can affect rates of microbial decomposition. Ecology 92:1471–1480.

German, D. P., M. N. Weintraub, A. S. Grandy, C. L. Lauber, Z. L. Rinkes, and S. D. Allison. 2011b. Optimization of hydrolytic and oxidative enzyme methods for ecosystem studies. Soil Biology and Biochemistry 43:1387–1397.

Haas, B. J., D. Gevers, A. M. Earl, M. Feldgarden, D. V. Ward, G. Giannoukos, D. Ciulla, D. Tabbaa, S. K. Highlander, E. Sodergren, B. Methe, T. Z. DeSantis, The Human Microbiome Consortium, J. F. Petrosino, R. Knight, and B. W. Birren. 2011. Chimeric 16S rRNA sequence formation and detection in Sanger and 454-pyrosequenced PCR amplicons. Genome Research 21:494–504.

Hartley, I. P., D. W. Hopkins, M. H. Garnett, M. Sommerkorn, and P. A. Wookey. 2008. Soil microbial respiration in arctic soil does not acclimate to temperature. Ecology Letters 11:1092–1100.

Hawkes, C. V., S. N. Kivlin, J. D. Rocca, V. Huguet, M. A. Thomsen, and K. B. Suttle. 2011. Fungal community responses to precipitation: FUNGAL CLIMATE RESPONSE. Global Change Biology 17:1637–1645.

Hill, B. H., C. M. Elonen, L. R. Seifert, A. A. May, and E. Tarquinio. 2012. Microbial enzyme stoichiometry and nutrient limitation in US streams and rivers. Ecological Indicators 18:540–551.

Hobbie, J. E., E. A. Hobbie, H. Drossman, M. Conte, J. C. Weber, J. Shamhart, and M. Weinrobe. 2009. Mycorrhizal fungi supply nitrogen to host plants in Arctic tundra and boreal forests: ^{15}N is the key signal. Canadian Journal of Microbiology 55:84–94.

Hodge, A., and A. H. Fitter. 2010. Substantial nitrogen acquisition by arbuscular mycorrhizal fungi from organic material has implications for N cycling. Proceedings of the National Academy of Sciences 107:13754–13759.

Högberg, M. N., and P. Högberg. 2002a. Extramatrical ectomycorrhizal mycelium contributes one-third of microbial biomass and produces, together with associated roots, half the dissolved organic carbon in a forest soil. New Phytologist 154:791–795.

Högberg, M. N., and P. Högberg. 2002b. Extramatrical ectomycorrhizal mycelium contributes one-third of microbial biomass and produces, together with associated roots, half the dissolved organic carbon in a forest soil. New Phytologist 154:791–795.

Hothorn, T., F. Bretz, and P. Westfall. 2008. Simultaneous inference in general parametric models. Biometrical Journal. Biometrische Zeitschrift 50:346–363.

Iovieno, P., and E. BÃ¥Ã¥th. 2008. Effect of drying and rewetting on bacterial growth rates in soil: Rewetting and bacterial growth in soil. FEMS Microbiology Ecology 65:400–407.

Jones, D. 2002. Simple method to enable the high resolution determination of total free amino acids in soil solutions and soil extracts. Soil Biology and Biochemistry 34:1893–1902.

Karhu, K., M. D. Auffret, J. A. J. Dungait, D. W. Hopkins, J. I. Prosser, B. K. Singh, J.-A. Subke, P. A. Wookey, G. I. Ågren, M.-T. Sebastià, F. Gouriveau, G. Bergkvist, P. Meir, A. T. Nottingham, N. Salinas, and I. P. Hartley. 2014. Temperature

sensitivity of soil respiration rates enhanced by microbial community response. Nature 513:81–84.
Koide, R. T., and T. Wu. 2003. Ectomycorrhizas and retarded decomposition in a Pinus resinosa plantation. New Phytologist 158:401–407.
Kõljalg, U., R. H. Nilsson, K. Abarenkov, L. Tedersoo, A. F. S. Taylor, M. Bahram, S. T. Bates, T. D. Bruns, J. Bengtsson-Palme, T. M. Callaghan, B. Douglas, T. Drenkhan, U. Eberhardt, M. Dueñas, T. Grebenc, G. W. Griffith, M. Hartmann, P. M. Kirk, P. Kohout, E. Larsson, B. D. Lindahl, R. Lücking, M. P. Martín, P. B. Matheny, N. H. Nguyen, T. Niskanen, J. Oja, K. G. Peay, U. Peintner, M. Peterson, K. Põldmaa, L. Saag, I. Saar, A. Schüßler, J. A. Scott, C. Senés, M. E. Smith, A. Suija, D. L. Taylor, M. T. Telleria, M. Weiss, and K.-H. Larsson. 2013. Towards a unified paradigm for sequence-based identification of fungi. Molecular Ecology 22:5271–5277.
Lawrence, D. M., K. W. Oleson, M. G. Flanner, P. E. Thornton, S. C. Swenson, P. J. Lawrence, X. Zeng, Z.-L. Yang, S. Levis, K. Sakaguchi, G. B. Bonan, and A. G. Slater. 2011. Parameterization improvements and functional and structural advances in Version 4 of the Community Land Model. Journal of Advances in Modeling Earth Systems 3.
LeBauer, D. S., and K. K. Treseder. 2008. Nitrogen limitation of net primary productivity in terrestrial ecosystems is globally distributed. Ecology 89:371–379.
Lindahl, B. D., W. de Boer, and R. D. Finlay. 2010. Disruption of root carbon transport into forest humus stimulates fungal opportunists at the expense of mycorrhizal fungi. The ISME journal 4:872–881.
Lindahl, B. D., K. Ihrmark, J. Boberg, S. E. Trumbore, P. Högberg, J. Stenlid, and R. D. Finlay. 2007a. Spatial separation of litter decomposition and mycorrhizal nitrogen uptake in a boreal forest. New Phytologist 173:611–620.
Lindahl, B. D., K. Ihrmark, J. Boberg, S. E. Trumbore, P. Högberg, J. Stenlid, and R. D. Finlay. 2007b. Spatial separation of litter decomposition and mycorrhizal nitrogen uptake in a boreal forest. New Phytologist 173:611–620.
Lindahl, B. D., and A. Tunlid. 2015. Ectomycorrhizal fungi - potential organic matter decomposers, yet not saprotrophs. New Phytologist 205:1443–1447.
Lipson, D. A., S. K. Schmidt, and R. K. Monson. 1999. Links between microbial population dynamics and nitrogen availability in an alpine ecosystem. Ecology 80:1623–1631.
Luo, Y., B. Su, W. S. Currie, J. S. Dukes, A. Finzi, U. Hartwig, B. Hungate, R. E. Mc MURTRIE, R. Oren, W. J. Parton, D. E. Pataki, M. R. Shaw, D. R. Zak, and C. B. Field. 2004. Progressive Nitrogen Limitation of Ecosystem Responses to Rising Atmospheric Carbon Dioxide. BioScience 54:731.
MacArthur, R. H., and E. R. Pianka. 1966. On optimal use of a patchy environment. The American Naturalist 100:603–609.
Mack, M. C., E. A. G. Schuur, M. S. Bret-Harte, G. R. Shaver, and F. S. Chapin. 2004. Ecosystem carbon storage in arctic tundra reduced by long-term nutrient fertilization. Nature 431:440–443.

McCune, B., and M. J. Mefford. 2011. PC-ORD Multivariate Analysis of Ecological Data. MjM Software, Gleneden Beach, Oregon, USA.
Melillo, J. M., A. D. McGuire, D. W. Kicklighter, B. Moore, C. J. Vorosmarty, and A. L. Schloss. 1993. Global climate change and terrestrial net primary production. Nature 363:234–240.
Melillo, J. M., P. A. Steudler, J. D. Aber, K. Newkirk, H. Lux, F. P. Bowles, C. Catricala, A. Magill, T. Ahrens, and S. Morisseau. 2002. Soil Warming and Carbon-Cycle Feedbacks to the Climate System. Science 298:2173–2176.
Moorhead, D. L., G. Lashermes, and R. L. Sinsabaugh. 2012. A theoretical model of C- and N-acquiring exoenzyme activities, which balances microbial demands during decomposition. Soil Biology and Biochemistry 53:133–141.
Muggeo, V. M. R. 2003. Estimating regression models with unknown break-points. Statistics in Medicine 22:3055–3071.
Muggeo, V. M. R. 2008. segmented: an R Package to Fit Regression Models with Broken-Line Relationships.
Oksanen, J., G. F. Blanchet, R. Kindt, P. Legendre, P. R. Minchin, R. B. O'Hara, G. L. Simpson, P. Solymos, M. H. H. Stevens, and H. Wagner. 2015. vegan: Community Ecology Package.
Orwin, K. H., M. U. F. Kirschbaum, M. G. St John, and I. A. Dickie. 2011. Organic nutrient uptake by mycorrhizal fungi enhances ecosystem carbon storage: a model-based assessment: Organic nutrient uptake enhances soil C. Ecology Letters 14:493–502.
Phillips, R. P., E. Brzostek, and M. G. Midgley. 2013. The mycorrhizal-associated nutrient economy: a new framework for predicting carbon-nutrient couplings in temperate forests. New Phytologist 199:41–51.
Phillips, R. P., A. C. Finzi, and E. S. Bernhardt. 2011. Enhanced root exudation induces microbial feedbacks to N cycling in a pine forest under long-term CO2 fumigation: Rhizosphere feedbacks in CO2-enriched forests. Ecology Letters 14:187–194.
Pinheiro, J., D. Bates, S. DebRoy, D. Sarkar, and R Core Team. 2014. {nlme}: Linear and Nonlinear Mixed Effects Models.
Pregitzer, K. S., A. J. Burton, D. R. Zak, and A. F. Talhelm. 2007. Simulated chronic nitrogen deposition increases carbon storage in Northern Temperate forests. Global Change Biology 0:071121035853002–???
Le Quéré, C., R. J. Andres, T. Boden, T. Conway, R. A. Houghton, J. I. House, G. Marland, G. P. Peters, G. R. van der Werf, A. Ahlström, R. M. Andrew, L. Bopp, J. G. Canadell, P. Ciais, S. C. Doney, C. Enright, P. Friedlingstein, C. Huntingford, A. K. Jain, C. Jourdain, E. Kato, R. F. Keeling, K. Klein Goldewijk, S. Levis, P. Levy, M. Lomas, B. Poulter, M. R. Raupach, J. Schwinger, S. Sitch, B. D. Stocker, N. Viovy, S. Zaehle, and N. Zeng. 2013. The global carbon budget 1959–2011. Earth System Science Data 5:165–185.
R Core Team. 2014. R: A language and environment for statistical computing. R Foundation for Statistical Computing, Vienna, Austria.

Read, D. J. 1991. Mycorrhizas in ecosystems. Experientia 47:376–391.
Read, D. J., and J. Perez-Moreno. 2003. Mycorrhizas and nutrient cycling in ecosystems–a journey towards relevance? New Phytologist 157:475–492.
Reich, P. B., D. F. Grigal, J. D. Aber, and S. T. Gower. 1997. Nitrogen mineralization and productivity in 50 hardwood and conifer stands on diverse soils. Ecology 78:335–347.
Rineau, F., D. Roth, F. Shah, M. Smits, T. Johansson, B. Canbäck, P. B. Olsen, P. Persson, M. N. Grell, E. Lindquist, I. V. Grigoriev, L. Lange, and A. Tunlid. 2012. The ectomycorrhizal fungus Paxillus involutus converts organic matter in plant litter using a trimmed brown-rot mechanism involving Fenton chemistry: Organic matter degradation by ectomycorrhizal fungi. Environmental Microbiology 14:1477–1487.
Rousk, J., and E. Bååth. 2011. Growth of saprotrophic fungi and bacteria in soil: Growth of saprotrophic fungi and bacteria in soil. FEMS Microbiology Ecology 78:17–30.
Rousk, J., S. D. Frey, and E. Bååth. 2012. Temperature adaptation of bacterial communities in experimentally warmed forest soils. Global Change Biology 18:3252–3258.
Schimel, J. P., and J. Bennett. 2004. Nitrogen mineralization: challenges of a changing paradigm. Ecology 85:591–602.
Schimel, J. P., and M. N. Weintraub. 2003. The implications of exoenzyme activity on microbial carbon and nitrogen limitation in soil: a theoretical model. Soil Biology and Biochemistry 35:549–563.
Schlesinger, W. H., and E. S. Bernhardt. 2012. Biogeochemistry: an analysis of global change. 3rd edition. Elsevier/Academic Press, New York.
Shepherd, M., A. Bhogal, G. Barrett, and C. Dyer. 2001. Dissolved organic nitrogen in agricultural soils: effects of sample preparation on measured values. Communications in Soil Science and Plant Analysis 32:1523–1542.
Shoval, O., H. Sheftel, G. Shinar, Y. Hart, O. Ramote, A. Mayo, E. Dekel, K. Kavanagh, and U. Alon. 2012. Evolutionary Trade-Offs, Pareto Optimality, and the Geometry of Phenotype Space. Science 336:1157–1160.
Sims, G. K., T. R. Ellsworth, and R. L. Mulvaney. 1995. Microscale determination of inorganic nitrogen in water and soil extracts. Communications in Soil Science and Plant Analysis 26:303–316.
Sinsabaugh, R. L., and J. J. Follstad Shah. 2012. Ecoenzymatic Stoichiometry and Ecological Theory. Annual Review of Ecology, Evolution, and Systematics 43:313–343.
Sinsabaugh, R. L., J. J. Follstad Shah, B. H. Hill, and C. M. Elonen. 2012. Ecoenzymatic stoichiometry of stream sediments with comparison to terrestrial soils. Biogeochemistry 111:455–467.
Sinsabaugh, R. L., B. H. Hill, and J. J. Follstad Shah. 2009. Ecoenzymatic stoichiometry of microbial organic nutrient acquisition in soil and sediment. Nature 462:795–798.

Sinsabaugh, R. L., C. L. Lauber, M. N. Weintraub, B. Ahmed, S. D. Allison, C. Crenshaw, A. R. Contosta, D. Cusack, S. Frey, M. E. Gallo, T. B. Gartner, S. E. Hobbie, K. Holland, B. L. Keeler, J. S. Powers, M. Stursova, C. Takacs-Vesbach, M. P. Waldrop, M. D. Wallenstein, D. R. Zak, and L. H. Zeglin. 2008. Stoichiometry of soil enzyme activity at global scale. Ecology Letters 11:1252–1264.

Steinweg, J. M., J. S. Dukes, E. A. Paul, and M. D. Wallenstein. 2013. Microbial responses to multi-factor climate change: effects on soil enzymes. Frontiers in Microbiology 4.

Sterner, R. W., and J. J. Elser. 2002. Ecological stoichiometry: the biology of elements from molecules to the biosphere. Princeton University Press, Princeton.

Talbot, J. M., T. D. Bruns, J. W. Taylor, D. P. Smith, S. Branco, S. I. Glassman, S. Erlandson, R. Vilgalys, H.-L. Liao, M. E. Smith, and K. G. Peay. 2014. Endemism and functional convergence across the North American soil mycobiome. Proceedings of the National Academy of Sciences 111:6341–6346.

Tedersoo, L., M. Bahram, S. Polme, U. Koljalg, N. S. Yorou, R. Wijesundera, L. V. Ruiz, A. M. Vasco-Palacios, P. Q. Thu, A. Suija, M. E. Smith, C. Sharp, E. Saluveer, A. Saitta, M. Rosas, T. Riit, D. Ratkowsky, K. Pritsch, K. Poldmaa, M. Piepenbring, C. Phosri, M. Peterson, K. Parts, K. Partel, E. Otsing, E. Nouhra, A. L. Njouonkou, R. H. Nilsson, L. N. Morgado, J. Mayor, T. W. May, L. Majuakim, D. J. Lodge, S. S. Lee, K.-H. Larsson, P. Kohout, K. Hosaka, I. Hiiesalu, T. W. Henkel, H. Harend, L. -d. Guo, A. Greslebin, G. Grelet, J. Geml, G. Gates, W. Dunstan, C. Dunk, R. Drenkhan, J. Dearnaley, A. De Kesel, T. Dang, X. Chen, F. Buegger, F. Q. Brearley, G. Bonito, S. Anslan, S. Abell, and K. Abarenkov. 2014. Global diversity and geography of soil fungi. Science 346:1256688–1256688.

Tedersoo, L., T. W. May, and M. E. Smith. 2010. Ectomycorrhizal lifestyle in fungi: global diversity, distribution, and evolution of phylogenetic lineages. Mycorrhiza 20:217–263.

Templer, P. H., and T. M. McCann. 2010. Effects of the Hemlock Woolly Adelgid on Nitrogen Losses from Urban and Rural Northern Forest Ecosystems. Ecosystems 13:1215–1226.

Thornton, P. E., S. C. Doney, K. Lindsay, J. K. Moore, N. Mahowald, J. T. Randerson, I. Fung, J.-F. Lamarque, J. J. Feddema, and Y.-H. Lee. 2009. Carbon-nitrogen interactions regulate climate-carbon cycle feedbacks: results from an atmosphere-ocean general circulation model. Biogeosciences 6:2099–2120.

Todd-Brown, K. E. O., F. M. Hopkins, S. N. Kivlin, J. M. Talbot, and S. D. Allison. 2012. A framework for representing microbial decomposition in coupled climate models. Biogeochemistry 109:19–33.

Torti, S. D., P. D. Coley, and T. A. Kursar. 2001. Causes and Consequences of Monodominance in Tropical Lowland Forests. The American Naturalist 157:141–153.

Treseder, K. K., and M. F. Allen. 2000. Mycorrhizal fungi have a potential role in soil carbon storage under elevated CO2 and nitrogen deposition. New Phytologist 147:189–200.

Treseder, K. K., T. C. Balser, M. A. Bradford, E. L. Brodie, E. A. Dubinsky, V. T. Eviner, K. S. Hofmockel, J. T. Lennon, U. Y. Levine, B. J. MacGregor, J. Pett-Ridge, and M. P. Waldrop. 2012. Integrating microbial ecology into ecosystem models: challenges and priorities. Biogeochemistry 109:7–18.

Vance, E. D., P. C. Brookes, and D. S. Jenkinson. 1987. An extraction method for measuring soil microbial biomass C. Soil Biology and Biochemistry 19:703–707.

Vitousek, P. M., and P. A. Matson. 1981. Nitrogen mineralization and nitrification potentials following clearcutting in the Hoosier National Forest, Indiana. Forest Science 27:781–791.

Waldrop, M. P., D. R. Zak, R. L. Sinsabaugh, M. Gallo, and C. Lauber. 2004. Nitrogen deposition modifies soil carbon storage through changes in microbial enzymatic activity. Ecological Applications 14:1172–1177.

Wallander, H., A. Ekblad, D. L. Godbold, D. Johnson, A. Bahr, P. Baldrian, R. G. Björk, B. Kieliszewska-Rokicka, R. Kjøller, H. Kraigher, C. Plassard, and M. Rudawska. 2013. Evaluation of methods to estimate production, biomass and turnover of ectomycorrhizal mycelium in forests soils – A review. Soil Biology and Biochemistry 57:1034–1047.

Wallander, H., L. O. Nilsson, D. Hagerberg, and U. Rosengren. 2003. Direct estimates of C:N ratios of ectomycorrhizal mycelia collected from Norway spruce forest soils. Soil Biology and Biochemistry 35:997–999.

Wallenstein, M. D., S. McNulty, I. J. Fernandez, J. Boggs, and W. H. Schlesinger. 2006. Nitrogen fertilization decreases forest soil fungal and bacterial biomass in three long-term experiments. Forest Ecology and Management 222:459–468.

Wallenstein, M. D., and M. N. Weintraub. 2008. Emerging tools for measuring and modeling the in situ activity of soil extracellular enzymes. Soil Biology and Biochemistry 40:2098–2106.

Wang, G., and W. M. Post. 2013. A note on the reverse Michaelis–Menten kinetics. Soil Biology and Biochemistry 57:946–949.

Wang, Q., G. M. Garrity, J. M. Tiedje, and J. R. Cole. 2007. Naive Bayesian Classifier for Rapid Assignment of rRNA Sequences into the New Bacterial Taxonomy. Applied and Environmental Microbiology 73:5261–5267.

Waring, B. G., C. Averill, and C. V. Hawkes. 2013a. Differences in fungal and bacterial physiology alter soil carbon and nitrogen cycling: insights from meta-analysis and theoretical models. Ecology Letters 16:887–894.

Waring, B. G., C. Averill, and C. V. Hawkes. 2013b. Differences in fungal and bacterial physiology alter soil carbon and nitrogen cycling: insights from meta-analysis and theoretical models. Ecology Letters 16:887–894.

Waring, B. G., and C. V. Hawkes. 2014. Short-Term Precipitation Exclusion Alters Microbial Responses to Soil Moisture in a Wet Tropical Forest. Microbial Ecology.

Watanabe, K., and K. Hayano. 1995. Seasonal variation of soil protease activities and their relation to proteolytic bacteria and *Bacillus* spp in paddy field soil. Soil Biology and Biochemistry 27:197–203.

White, T. J., T. Bruns, S. Lee, and J. W. Taylor. 1990. Amplification and direct sequencing of fungal ribosomal RNA genes for phylogenetics. PCR Protocols: A Guide to Methods and Applications. Academic Press, Inc., New York.

Wieder, W. R., G. B. Bonan, and S. D. Allison. 2013. Global soil carbon projections are improved by modelling microbial processes. Nature Climate Change 3:909–912.

Wieder, W. R., C. C. Cleveland, W. K. Smith, and K. Todd-Brown. 2015. Future productivity and carbon storage limited by terrestrial nutrient availability. Nature Geoscience.